Astronomy & Astrophysics manuscript no. art-acc
(DOI: will be inserted by hand later)

June 28, 2004

C, S, Zn and Cu abundances in planet-harbouring stars*

A. Ecuvillon,[1] G. Israelian,[1] N. C. Santos,[2,3] M. Mayor,[3] V. Villar[4] and G. Bihain[1]

[1] Instituto de Astrofísica de Canarias, E-38200 La Laguna, Tenerife, Spain
[2] Centro de Astronomia e Astrofisica de Universidade de Lisboa, Observatorio Astronomico de Lisboa, Tapada de Ajuda, 1349-018 Lisboa, Portugal
[3] Observatoire de Genève, 51 ch. des Maillettes, CH–1290 Sauverny, Switzerland
[4] Departamento de Astrofísica, Fac. de Físicas, Universidad Complutense de Madrid, Ciudad Universitaria, E-28040 Madrid, Spain

Received 22 April 2004 / Accepted 17 June 2004

Abstract. We present a detailed and uniform study of C, S, Zn and Cu abundances in a large set of planet host stars, as well as in a homogeneous comparison sample of solar-type dwarfs with no known planetary-mass companions. Carbon abundances were derived by EW measurement of two C I optical lines, while spectral syntheses were performed for S, Zn and Cu. We investigated possible differences in the behaviours of the volatiles C, S and Zn and in the refractory Cu in targets with and without known planets in order to check possible anomalies due to the presence of planets. We found that the abundance distributions in stars with exoplanets are the high [Fe/H] extensions of the trends traced by the comparison sample. All volatile elements we studied show [*X*/Fe] trends decreasing with [Fe/H] in the metallicity range $-0.8 <$ [Fe/H] < 0.5, with significantly negative slopes of -0.39 ± 0.04 and -0.35 ± 0.04 for C and S, respectively. A comparison of our abundances with those available in the literature shows good agreement in most cases.

Key words. stars: abundances – stars: chemically peculiar – stars: evolution – planetary systems – solar neighbourhood

1. Introduction

Since the first success in the search for exoplanets with the discovery of the planet orbiting 51 Peg (Mayor & Queloz 1995), studies on the formation and evolution of planetary systems have increased. Several spectroscopic analyses of stars with planets have recently been carried out. Most of them used iron as the reference element (Gonzalez 1997; Murray & Chaboyer 2002; Laws et al. 2003; Santos et al. 2001, 2003b, 2004a; for a review see Santos et al. 2003a), while only a few studies determined abundance trends for other metals (Gonzalez & Laws 2000; Gonzalez et al. 2001; Santos et al. 2000; Bodaghee et al. 2003; Takeda et al. 2001; Sadakane et al. 2002; for a review see Israelian 2003b).

One of the most remarkable results is that planet-harbouring stars are on average more metal-rich than solar-type disc stars (Gonzalez 1997; Gonzalez et al. 2001; Laws et al. 2003; Santos et al. 2001, 2003b, 2004a). Two main explanations have been suggested for linking this metallicity excess with the presence of planets. The first of these, the "self-enrichement" hypothesis, attributes the origin of the observed overabundance of metals to the accretion of large amounts of metal-rich H- and He-depleted rocky planetesimal materials on to the star (Gonzalez 1997). The opposite view, the "primordial" hypothesis, considers the metallicity enhancement to be caused by the high metal content of the protoplanetary cloud from which the planetary system formed (Santos et al. 2000, 2001). Discriminating between these two possibilities will help in understanding how planetary systems form.

Light elements may give fundamental information about the mixing, diffusion and angular momentum history of exoplanets hosts, as well as stellar activity caused by interaction with exoplanets (Santos et al. 2002, 2004b; Israelian et al. 2004). Studies of Be, Li and the isotopic ratio ^{6}Li/^{7}Li could give evidences to distinguish between different planet formation theories (Sandquist et al. 2002).

Murray & Chaboyer (2002) concluded that an accretion of 5.0 $M_\oplus$ of iron while on the main sequence would explain the overabundance of metals found in planet host stars. On the other hand, Pinsonneault et al. (2001) rejected the "self-enrichement" scenario since the metallicity enhancement does not show the expected $T_{\rm eff}$ dependence; recent results by Vauclair (2004) may have refuted, however, this argument.

Send offprint requests to: e-mail: aecuvill@ll.iac.es

* Based on observations collected at the La Silla Observatory, ESO (Chile), with the CORALIE spectrograph at the 1.2-m Euler Swiss telescope and with the FEROS spectrograph at the 1.52-m and 2.2-m ESO telescopes, at the Paranal Observatory, ESO (Chile), using the UVES spectrograph at the VLT/UT2 Kueyen telescope, and with the UES and SARG spectrographs at the 4-m William Hershel Telescope (WHT) and at the 3.5-m TNG telescope, respectively, both at La Palma (Canary Islands).

Furthermore, several studies have shown that planetary frequency is rising as a function of [Fe/H] (Santos et al. 2001, 2004a; Reid 2002), result which seems to support the primordial metallicity enhancement scenario. However, evidences of pollution have been found for a few cases (Israelian et al. 2001, 2003a; Laws & Gonzalez 2001).

Abundance trends of different elements may provide important clues to the question. Volatile elements (with low condensation temperature T_C) are expected to be deficient in accreted materials because of the high temperatures near the star. Therefore, the "self-enrichement" scenario should lead to a relative overabundance of refractories, such as the α-elements Si, Mg, Ca, Ti and the iron-group elements compared to volatiles, such as CNO, S and Zn. Smith et al. (2001) found a small subset of planet host stars which bore this accretion signature since these stars exhibited an accentuated trend of increasing $[X/\mathrm{H}]$ with increasing T_C for a given element X. Nevertheless, subsequent studies have obtained a similar behaviour in volatiles as in refractory elements (Takeda et al. 2001; Sadakane et al. 2002).

Other evidence in favour of a "primordial" high metallicity has been provided by several studies, which conclude that the abundances of volatiles in planet host stars do not reveal significant differences from those in field dwarfs of the same metallicity (Santos et al. 2000; Gonzalez et al. 2001; Takeda et al. 2001; Sadakane et al. 2002). However, all these authors used inhomogeneous comparison samples of field dwarfs from the literature, which could be a source of systematic errors. A sample of stars with no known planets has been prepared by Santos et al. (2001) and analysed in the same way as the planet host set in several studies of the stellar and kinematic parameters of stars with planets (Santos et al. 2003b) and about their metal-rich nature (Santos et al. 2001, 2004a). Other uniform and unbiased comparisons have been carried out for abundances of elements other than iron – some α- and Fe-group elements (Bodaghee et al. 2003) and the volatile nitrogen (Ecuvillon et al. 2004) – and conclude that the abundance trends observed in planet host stars are almost identical to those in the comparison sample.

Sulphur is a volatile α element which behaves as true primary; it is well established that it is produced mainly by Type II supernovae (SNe II) of massive stars (e.g. Timmes, Woosley & Weaver 1995; Carretta, Gratton & Sneden 2000). For Cu and Zn the situation is rather confused; massive ($M>8M_\odot$), low- ($M<4M_\odot$) and intermediate-mass stars ($4M_\odot<M<8M_\odot$) are likely contributors, although their relative weights are still uncertain (e.g. Luck & Bond 1985; Sneden et al. 1991; Mishenina et al. 2002; Bihain et al. 2004). A number of different production sites have been suggested for carbon: supernovae, novae, Wolf-Rayet stars, intermediate- and low-mass stars. Recently, Kobulnicky & Skillman (1998) concluded that low- and intermediate- mass stars are the significant contributors of carbon. On the other hand, Prantzos et al. (1994) and Gustafsson et al. (1999) found massive stars to be significant sites for the production of carbon. At the present the situation is not clear.

This work presents a systematic, uniform and detailed study of the volatile elements C, S and Zn and of the refractory Cu in two large samples, a set of planet-harbouring stars and a volume-limited comparison sample of stars with no known planetary mass companions. We studied C, S, Zn and Cu abundances in several optical lines, by measuring EW in the case of carbon and by the synthesis technique for the other elements. We compare our results with those of other recent studies (Santos et al. 2000; Gonzalez et al. 2001; Takeda et al. 2001; Sadakane et al. 2002).

Table 1. Observing log for the new set of data. The S/N ratio is provided at 6050 Å and 5375 Å

Star	V	Obser. run	S/N	Date
HD 7570	5.0	UVES	850	July 2001
HD 9826	4.1	UES	500	Feb. 2001
HD 16141	6.8	UES	800	Oct. 2001
HD 17051	5.4	UVES	950	July 2001
HD 19994	5.1	UVES	1100	Aug. 2001
HD 22049	3.7	UES	500	Oct. 2001
HD 52265	6.3	UVES	1200	Mar. 2001
HD 75289	6.4	UVES	1000	Mar. 2001
HD 82943	6.5	UVES	950	Mar. 2001
HD 89744	5.7	UES	680	Feb. 2001
HD 108147	7.0	UVES	950	Mar. 2001
HD 114762	7.3	UVES	1350	Mar. 2001
HD 120136	4.5	UVES	1100	Mar. 2001
HD 121504	7.6	UVES	900	Mar. 2001
HD 195019	6.9	UES	800	Oct. 2001
HD 209458	7.7	UVES	1100	June 2001
HD 217107	6.2	UES	500	Oct. 2001

2. Observations

Most of the analysed spectra were collected during several observational campaigns with the CORALIE spectrograph on the 1.2 m Euler Swiss telescope, the FEROS spectrograph on the 2.2 m ESO/MPI telescope (both at La Silla, Chile), the UVES spectrograph on the VLT/UT2 Kueyen telescope (Paranal Observatory, ESO, Chile), the SARG spectrograph on the 3.5 m TNG and the UES spectrograph on the 4.2 m WHT (both at the Roque de los Muchachos Observatory, La Palma, Spain). Part of these data were used in previous articles to derive precise stellar parameters (Santos et al. 2001, 2003b, 2004a) and abundances of C, O, S, Si, Ca and Ti (Santos et al. 2000), as well as to study trends of nine refractory elements (Bodaghee et al. 2003) and of the volatile nitrogen (Ecuvillon et al. 2004). We refer the reader to these papers for a description of the data.

New spectra with high S/N ratios from the UVES and UES spectrographs, on the VLT/UT2 Kueyen telescope (Paranal Observatory, ESO, Chile) and on the 4.2 m WHT (Roque de los Muchachos Observatory, La Palma, Spain), respectively, were used. These are listed in Table 1. The S/N ratios for these spectra are in most cases higher than 800 at a resolution of 55000 and 110000 for the UES and the UVES spectrograph, respectively.

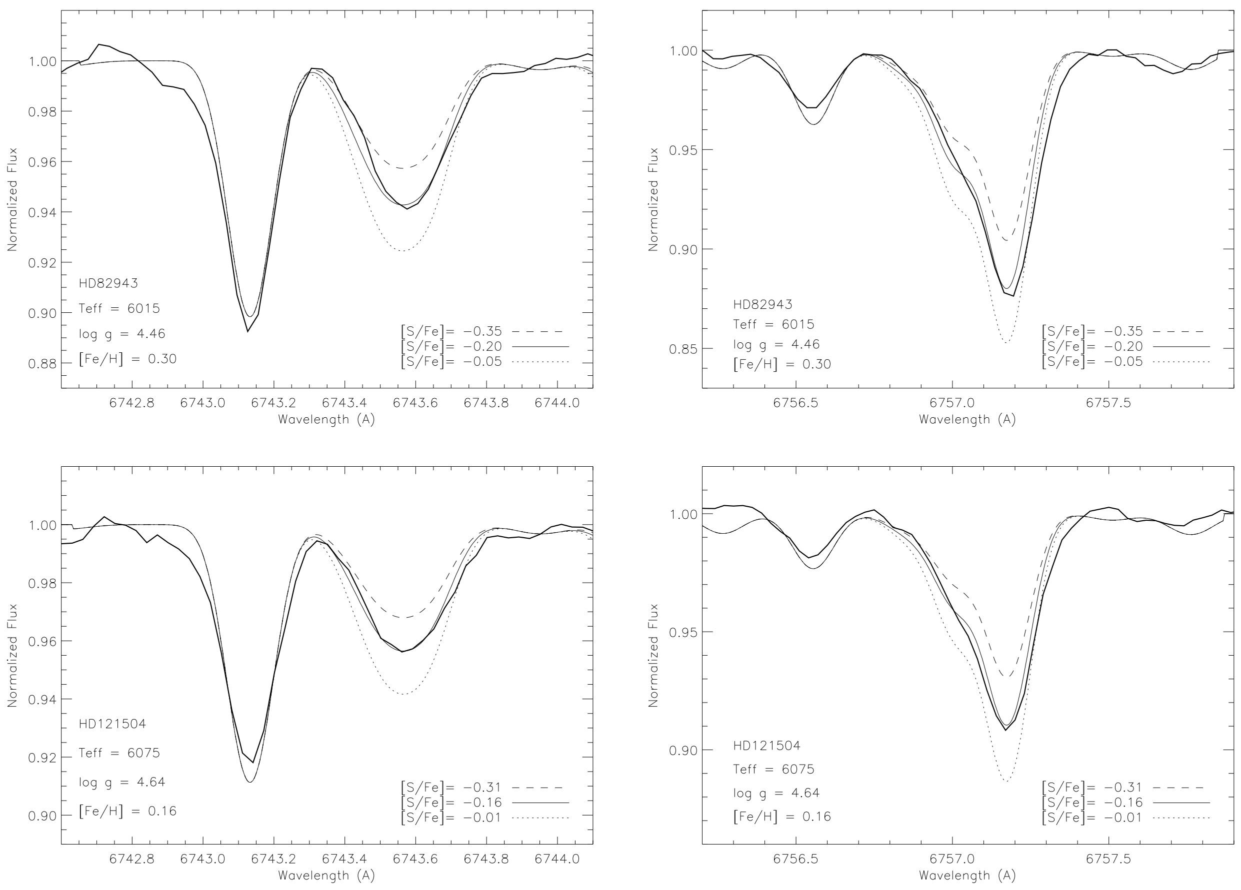

Fig. 1. The observed spectrum (thick solid line) and three synthetic spectra (dotted, dashed and solid lines) for different values of [S/Fe], in the spectral regions 6742.6–6744.1 Å and 6756.2–6757.9 Å, for two targets.

3. Analysis

The abundance analysis was carried out in standard local thermodinamic equilibrium (LTE) using a revised version of the spectral synthesis code MOOG (Sneden 1973) and a grid of Kurucz (1993) ATLAS9 atmospheres. All the atmospheric parameters, $T_{\rm eff}$, $\log g$, ξ_t and [Fe/H], and the corresponding uncertainties, were taken from Santos et al. (2004a). The adopted solar abundances for carbon, sulphur, zinc, copper and iron were respectively $\log \epsilon\,(\mathrm{C})_\odot = 8.56$ dex, $\log \epsilon\,(\mathrm{S})_\odot = 7.21$ dex , $\log \epsilon\,(\mathrm{Zn})_\odot = 4.60$ dex, $\log \epsilon\,(\mathrm{Cu})_\odot = 4.21$ dex (Anders & Grevesse 1989) and $\log \epsilon\,(\mathrm{Fe})_\odot = 7.47$ dex (as used in Santos et al. 2004a).

Carbon abundance analysis was carried out by EW measurement of two C I lines 5380.3 Å and at 5052.2 Å. Wavelength and excitation energies of the lower level were taken from VALD (Kupka et al. 1999) and solar gf values were computed using EWs (21.0 mÅ and 34.2 mÅ, respectively) obtained from the Kurucz Solar Atlas (Kurucz et al. 1984), and a solar model with $T_{\rm eff} = 5777$ K, $\log g = 4.44$ and $\xi_t = 1.0\,\mathrm{km\,s^{-1}}$. All the adopted parameters for each spectral line are presented in Table 2. EWs were determined by Gaussian fitting using the SPLOT task of IRAF and abundances were computed with the ABFIND driver of MOOG.

Sulphur, zinc and copper abundances were derived by fitting synthetic spectra to the data. For sulphur, we analysed two S I features: the first at 6743.5 Å consisting of three S I lines, at 6743.44 Å, 6743.53 Å and at 6743.64 Å, and the second at 6757.1 Å consisting of two S I lines, at 6757.01 Å and at 6757.18 Å. Fits were carried out in the spectral regions 6742.5–6744.5 Å and 6756.0–6758.0 Å. The line lists for each spectral region were taken from VALD (Kupka et al. 1999) and $\log gf$ values were slightly modified in order to achieve a good fit to the Kurucz Solar Atlas (Kurucz et al. 1984). The adopted atomic data are listed in Table 2. For the instrumental broadening we used a Gaussian function with FWHM of 0.07 Å and 0.11 Å, depending on the instrumental resolution, and a rotational broadening function with $v \sin i$ values from the CORALIE database. For targets without a CORALIE $v \sin i$ determination, we chose the $v \sin i$ values which fitted the best the spectral lines in the synthesized regions. These values were between 1 and 5 $\mathrm{km\,s^{-1}}$, since all our targets are slow rotators. Two examples of the fitting of the two features are shown in Figure 1. The red side of the S I feature at 6757 Å could not be perfectly reproduced because of an unknown feature between 6757.25 and 6757.45 Å (there are no spectral lines in the VALD database at these wavelengths). Our differential analysis relative to the Sun cancels out this source of uncertainty since all our targets are affected in the same way as the Sun. Moreover, we have verified that an *EW* analysis yields the same final

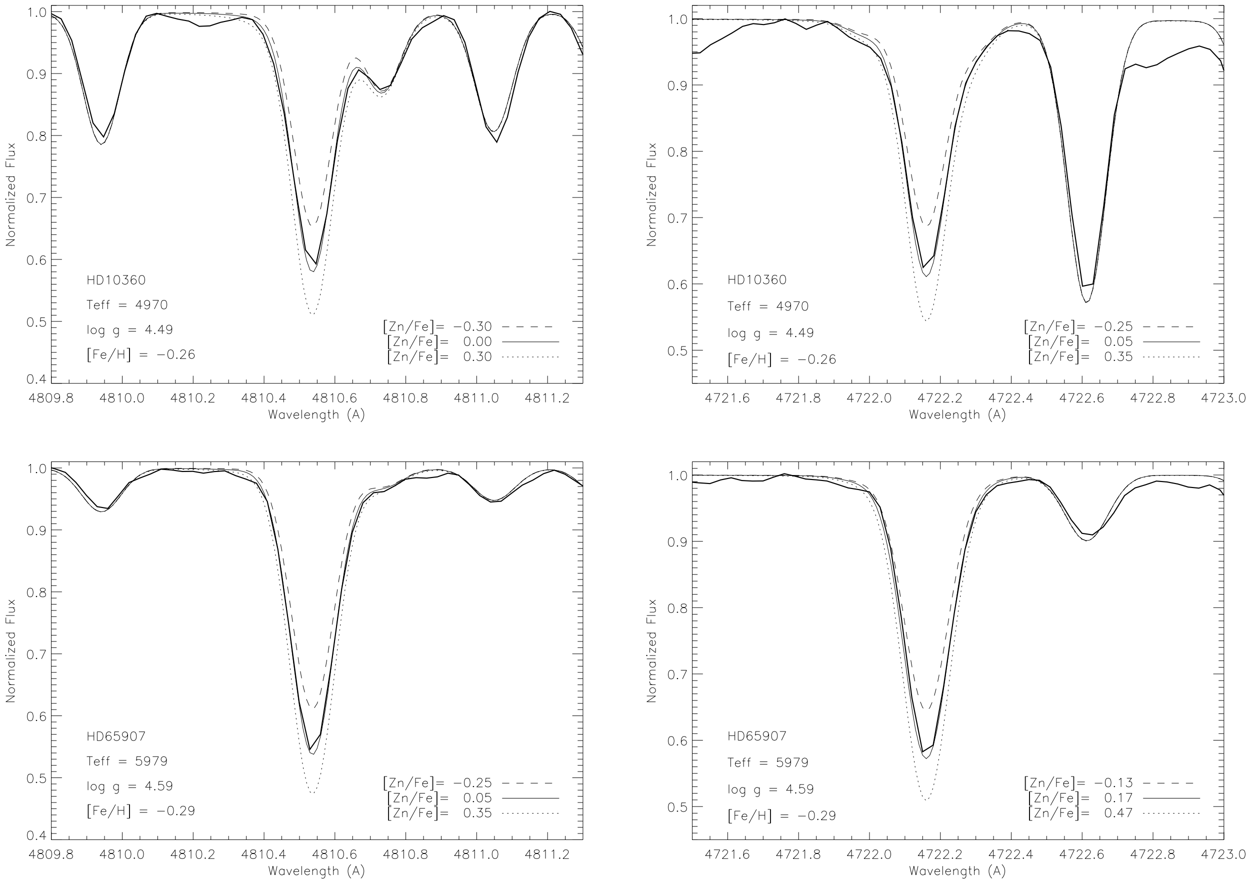

Fig. 2. The observed spectrum (thick solid line) and three synthetic spectra (dotted, dashed and solid lines) for different values of [Zn/Fe], in the spectral regions 4809.8–4811.3 Å and 4721.5–4723.0 Å, for two targets.

abundances, and therefore we consider this effect to be negligible.

Zinc abundances were derived from the two Zn I lines at 4810.5 Å and at 4722.2 Å. We computed 5Å wide synthetic spectra. The atomic lists for elements other than zinc were provided by VALD (Kupka et al. 1999), while atomic data for the Zn I lines were taken from Gurtovenko & Kostyk (1989). Copper abundances were derived from the Cu I lines at 5218.2 Å and at 5782.1 Å, by the synthesis of the spectral regions 5213–5220 Å and 5780–5785Å. The atomic lists for elements other than copper were provided by VALD (Kupka et al. 1999), while atomic data (hyperfine structure components) for the Cu I lines were taken from Steffen (1985). A differential analysis relative to the Sun was carried out for the two elements. Some wavelengths were slightly modified in order to fit the solar spectrum better. Table 2 presents the adopted values for both elements. Figures 2 and 3 show two examples of fits for the Zn I and Cu I lines, respectively.

Uncertainties in the atmospheric parameters are of the order of 50 K in $T_{\rm eff}$, 0.12 dex in $\log g$, 0.08 km s^{-1} in ξ_t and 0.05 dex in [Fe/H] (see Santos et al. 2004a). We estimated the effect of changes in atmospheric parameters on the resulting abundances in the following way. For each atmospheric parameter, we selected a set of three stars having similar values of all the parameters, excepting the considered one, which must vary within the sample. We then tested abundance sensitivity to changes in the parameter ($\pm$100 K for $T_{\rm eff}$, $\pm$0.3 dex for $\log g$ and [Fe/H], $\pm$0.5 km s^{-1} for ξ_t). The results are shown in Table 3. Uncertainties in the abundances of all the elements were determined adding in quadrature the dispersion of each abundance from the mean value, 0.05 dex of the continuum determination and the errors due to the abundance sensitivities to changes in the atmospheric parameters.

Dependences on $T_{\rm eff}$ and on $\log g$ of [C/Fe], [S/Fe], [Zn/Fe] and [Cu/Fe] are represented in Fig. 4, Fig. 5, Fig. 6 and Fig. 7, respectively. We note that no characteristic trends appear in any of the cases. This means that our results are almost free from systematic errors. Only in the case of Zn does [Zn/Fe] decrease for $T_{\rm eff}$ greater than 6000 K. This could be due to an NLTE effect, usually not very strong in metal-rich stars for complex atoms such as iron (see Edvardsson et al. 1993; Thévenin & Idiart 1999). We verified that using only stars with $T_{\rm eff}$ lower than 6000 K would not change the resulting trends.

4. Results

Several studies have been recently published about abundances of elements other than iron in planet host stars (e.g. Santos et al. 2000, 2002; Gonzalez et al. 2001; Takeda et al. 2001; Sadakane et al. 2002; Bodaghee et al. 2003; Israelian et al.

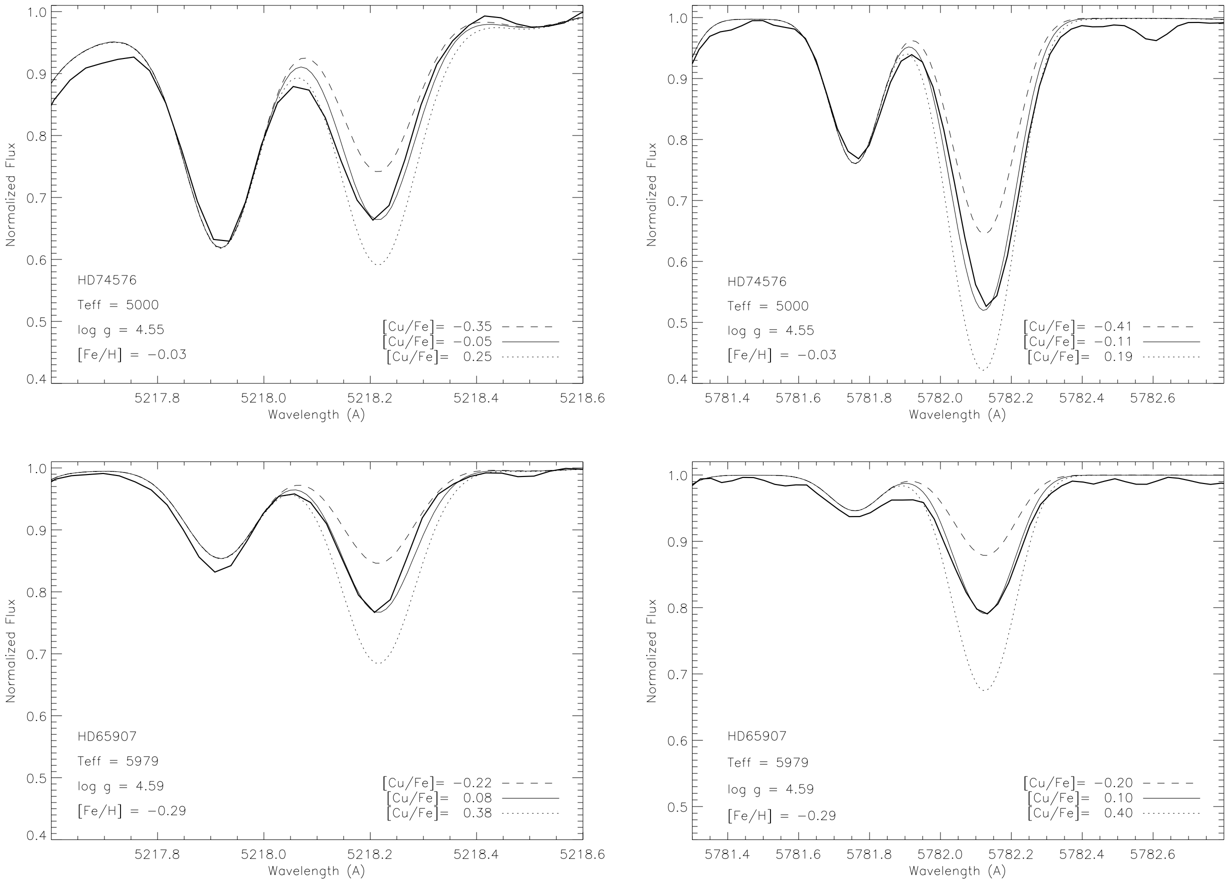

Fig. 3. The observed spectrum (thick solid line) and three synthetic spectra (dotted, dashed and solid lines) for different values of [Cu/Fe], in the spectral regions 5217.6–5218.6 Å and 5781.3–5782.8 Å, for two targets.

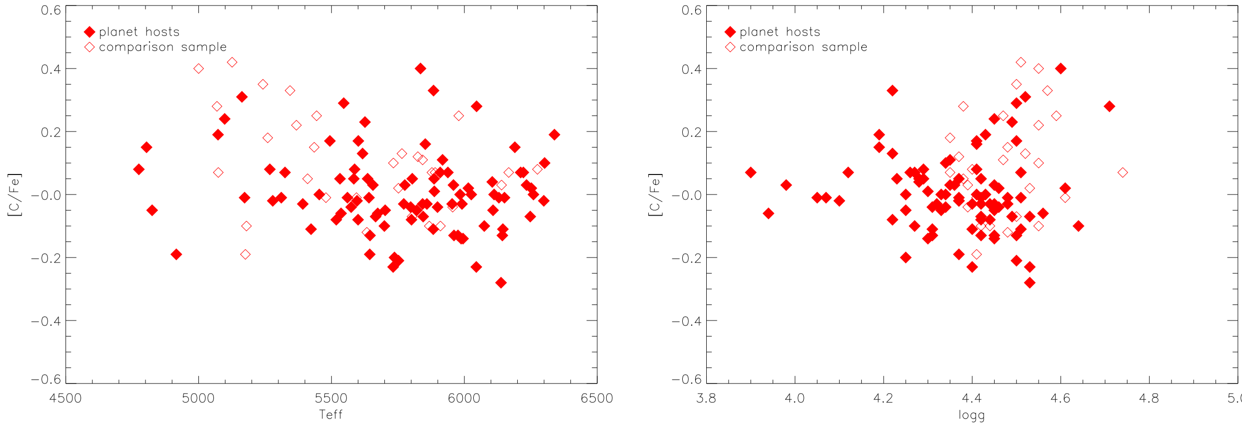

Fig. 4. [C/Fe] vs. T_{eff} and $\log g$. Filled and open symbols represent planet host and comparison sample stars, respectively.

2004; Ecuvillon et al. 2004). Studies concerning such volatile elements as CNO, S and Zn were carried out, but most of them did not count on a large set of planet-harbouring targets and a homogeneous comparison sample of stars without known planetary companions.

Santos et al. (2000) compared the abundances of C, O and S for eight planet host stars with results for field dwarfs from the literature without finding significant differences. They pointed out the need to use a homogeneous comparison sample of stars without planetary mass companions. Also Gonzalez et al. (2001) found no deviation of the C and O abundances of twenty planet hosts from the trends traced by field stars taken from the literature. Takeda et al. (2001) and Sadakane et al. (2002) presented abundances of twelve and nineteen elements, respectively, among which the volatiles C, N, O, S and Zn and the refractory Cu, for fourteen and twelve planet-harbouring

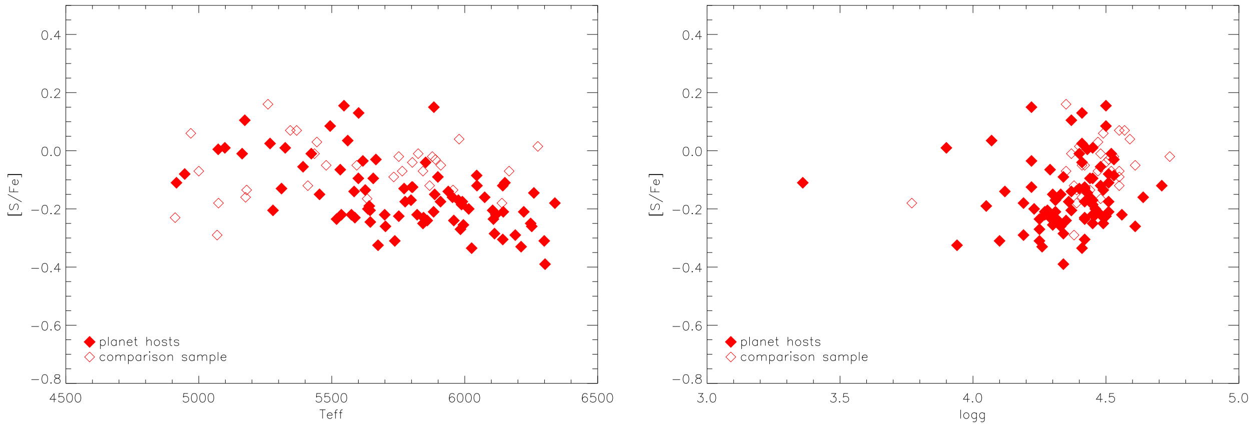

Fig. 5. [S/Fe] vs. $T_{\rm eff}$ and $\log g$. Filled and open symbols represent planet host and comparison sample stars, respectively.

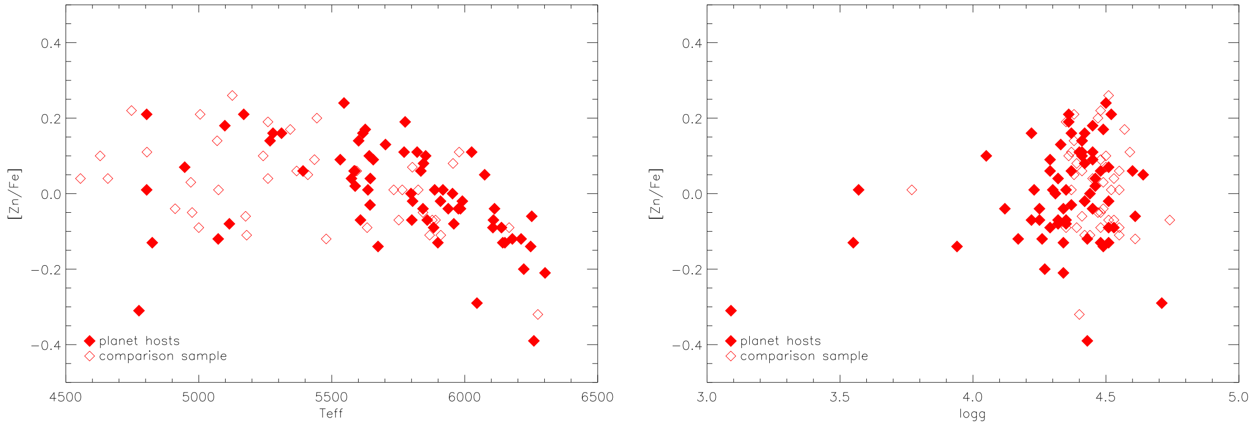

Fig. 6. [Zn/Fe] vs. $T_{\rm eff}$ and $\log g$. Filled and open symbols represent planet host and comparison sample stars, respectively.

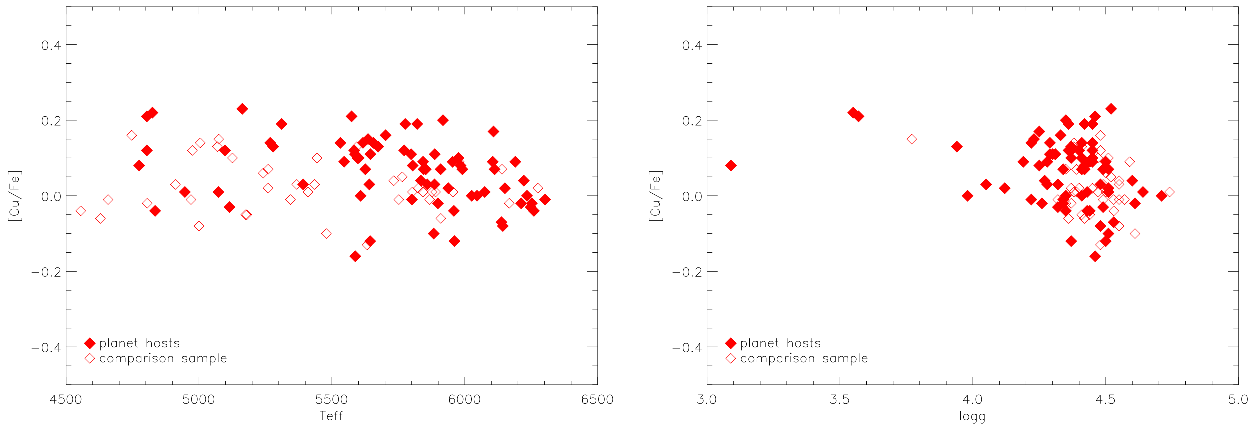

Fig. 7. [Cu/Fe] vs. $T_{\rm eff}$ and $\log g$. Filled and open symbols represent planet host and comparison sample stars, respectively.

stars, respectively. Their results revealed no anomalies between planet host and comparison samples. Ecuvillon et al. (2004) presented a homogeneous analysis of N abundances in 91 solar-type stars, 66 with and 25 without known planets, and confirmed that the two samples show the same behaviour.

In this paper we analysed two optical lines of C I in 91 targets with planets and in 31 comparison sample stars. All atmospheric parameters, EW values with uncertainties and abundance results for both samples are listed in Tables 6, 6 and 6. For sulphur, zinc and copper, we synthesized two optical lines in 84, 68 and 73 planet host stars, and in 31, 41 and 41 comparison sample stars, respectively. Atmospheric parameters, abundance results and the corresponding uncertainties, are listed in Tables 6 to 6.

Table 3. Sensitivity of the abundances of C, S, Zn and Cu to changes of 100 K in effective temperature, 0.3 dex in gravity and metallicity, and 0.5 km s^{-1} in microturbulence

	Star ($T_{\rm eff}$; log g ; [Fe/H] ; ξ_t)	HD 22049 (5073; 4.43; -0.13; 1.05)	HD 168746 (5601; 4.41; -0.08; 0.99)	HD 136118 (6222; 4.27; -0.04; 1.79)
C:	$\Delta T_{\rm eff} = \pm 100$ K	∓0.09	∓0.07	∓0.05
S:	$\Delta T_{\rm eff} = \pm 100$ K	∓0.10	∓0.10	∓0.05
Zn:	$\Delta T_{\rm eff} = \pm 100$ K	±0.03	±0.04	±0.05
Cu:	$\Delta T_{\rm eff} = \pm 100$ K	±0.03	±0.05	±0.05

	Star ($T_{\rm eff}$; log g ; [Fe/H]; ξ_t)	HD 10697 (5641; 4.05; 0.14; 1.13)	HD 16141 (5801; 4.22; 0.15; 1.34)	HD 28185 (5656; 4.45; 0.22; 1.01)
C:	$\Delta \log g = \pm 0.3$ dex	∓0.10	∓0.10	∓0.10
S:	$\Delta \log g = \pm 0.3$ dex	∓0.10	∓0.10	∓0.10
Zn:	$\Delta \log g = \pm 0.3$ dex	±0.07	±0.07	±0.06
Cu:	$\Delta \log g = \pm 0.3$ dex	±0.02	±0.03	±0.03

	Star ($T_{\rm eff}$; log g ; [Fe/H]; ξ_t)	HD 6434 (5835; 4.60; -0.52; 1.53)	HD 95128 (5954; 4.44; 0.06; 1.30)	HD 4203 (5636; 4.23; 0.40; 1.12)
C:	Δ[Fe/H]= ±0.3 dex	∓0.03	∓0.02	∓0.02
S:	Δ[Fe/H] = ±0.3 dex	∓0.00[1]	∓0.00[1]	∓0.00[1]
Zn:	Δ[Fe/H] = ±0.3 dex	∓0.20	∓0.20	∓0.20
Cu:	Δ[Fe/H] = ±0.3 dex	∓0.30	∓0.20	∓0.20

	Star ($T_{\rm eff}$; log g ; [Fe/H]; ξ_t)	HD 49674 (5644; 4.37; 0.33; 0.89)	HD 73256 (5518; 4.42; 0.26; 1.22)	HD 19994 (6190; 4.19; 0.24; 1.54)
C:	$\Delta\xi_t = \pm 0.5$km s^{-1}	∓0.01	∓0.01	∓0.01
S:	$\Delta\xi_t = \pm 0.5$km s^{-1}	∓0.00[1]	∓0.00[1]	∓0.00[1]
Zn:	$\Delta\xi_t = \pm 0.5$km s^{-1}	∓0.10	∓0.10	∓0.10
Cu:	$\Delta\xi_t = \pm 0.5$km s^{-1}	∓0.10	∓0.10	∓0.10

[1] These sensitivities are based on the method described in Section 3. The values can be slightly larger if more explicit calculations are carried out.

Figure 8 presents [C/H] and [C/Fe] as functions of [Fe/H]. Both samples, stars with and without planets, behave quite similarly. Since targets with planets are on average more metal rich than comparison sample stars, their abundance distributions correspond to the extensions of the comparison sample trends at high [Fe/H]. Planet host stars do not present anomalies in carbon abundances with respect to comparison sample dwarfs.

Similar results are obtained for sulphur and zinc. Figures 9 and 10 show the [X/H] and [X/Fe] vs. [Fe/H] plots for the two elements. The abundance trends of sulphur and zinc in planet host stars are similar to those of the comparison sample. In fact, no discontinuity is seen in the overlap region of both samples.

[X/Fe] vs. [Fe/H] plots for the three volatiles show decreasing trends with increasing [Fe/H]. Although this effect is more evident for [C/Fe] and [S/Fe] than for [Zn/Fe], they all show a negative slope . This means that, unlike nitrogen (see Ecuvillon et al. 2004), none of these elements keeps pace with iron; an excess of carbon, sulphur and zinc exists in the more metal-poor tail with respect to stars with high [Fe/H]. Since no differences appear to be related to the presence of planets, the observed slopes may be a by-product of Galactic chemical evolution. However, no detailed models are available to explain trends such as these.

[Cu/H] and [Cu/Fe] vs. [Fe/H] trends are provided in Figure 11. No discontinuities appear between the two samples. In the [Cu/Fe] vs. [Fe/H] plot, the planet host star set seems to produce a steeper fit than that corresponding to the comparison sample. Although this may be seen as a signature of the presence of planets, it seems more likely that the [Cu/Fe] slope

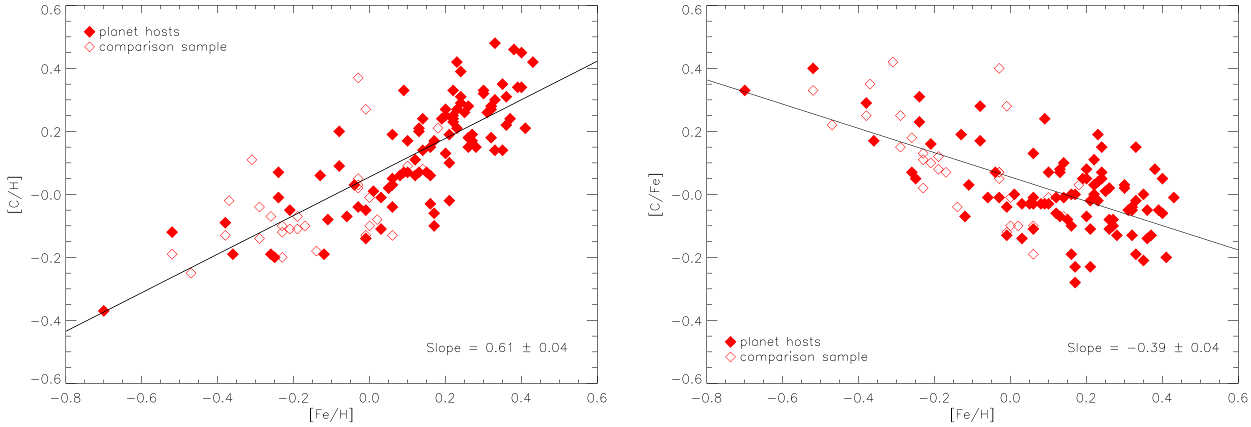

Fig. 8. [C/H] and [C/Fe] vs. [Fe/H] plots. Filled and open symbols represent planet host and comparison sample stars, respectively. Linear least-squares fits to both samples together are represented and slope values are indicated at the bottom of each plot.

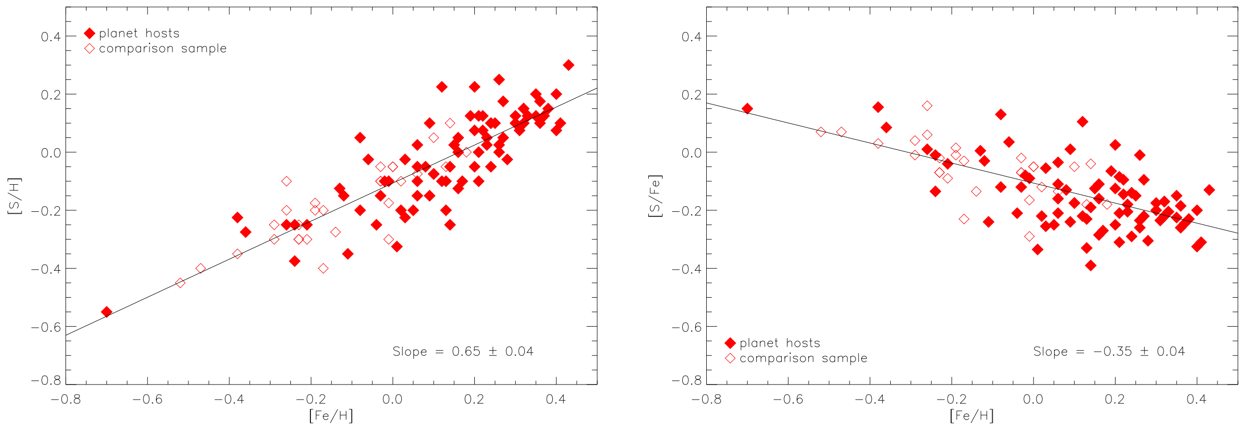

Fig. 9. [S/H] and [S/Fe] vs. [Fe/H] plots. Filled and open symbols represent planet host and comparison sample stars, respectively. Linear least-squares fits to both samples together are represented and slope values are indicated at the bottom of each plot.

increases at [Fe/H] > 0.1, and that its relation to the presence of planets is solely due to the high metallicity of the parent stars. The [Cu/Fe] trend corresponding to both samples is on average slightly overabundant with respect to [Fe/H].

The [X/H] distributions for the four elements are presented in Figure 12. Volatile (C, S and Zn) distributions differ in their shapes. The planet host distributions are strongly asymmetrical, with peaks at high [X/H]. The comparison samples show different behaviours: the same asymmetric distribution for sulphur and a mirror shape for carbon. In the case of zinc, the comparison sample distribution looks more symmetrical. The [Cu/H] distributions for the two sets, stars with and without planets, present similar shapes, both quite symmetric. The cumulative distributions show that differences between planet host and comparison sample stars are statistically significant.

The average values of [X/H] for the samples with and without planets for each element, as well as the rms dispersions and the differences between the mean [X/H] values, are listed in Table **??**. The differences vary from 0.16 to 0.31 dex. These discrepancies are not very significant because of the high dispersion around the mean value.

We note that the differences between average values of [X/H] for the two samples are smaller for carbon and sulphur than for zinc and copper. For nitrogen, another volatile element, a difference of the order of 0.3 dex was found between the average [N/H] values for planet host and comparison sample stars (Ecuvillon et al. 2004). Even though these discrepancies are not statistically significant, we cannot completely exclude that this characteristic, if confirmed, may be related with the different condensation temperatures of the elements.

5. Comparison with the literature

Previous studies concerning abundances of refractory and volatiles elements (see Sect. 4) have analysed planet host stars common to our study. In order to carry out a homogeneous comparison, we gathered all these abundance results and scaled them to our atmospheric parameters using the published sensitivities for each atomic line.

Santos et al. (2000), Gonzalez et al. (2001), Takeda et al. (2001) and Sadakane et al. (2002) analysed one of the two C I lines we used to compute carbon abundances, the C I line at 5380 Å. We could therefore directly compare the measured

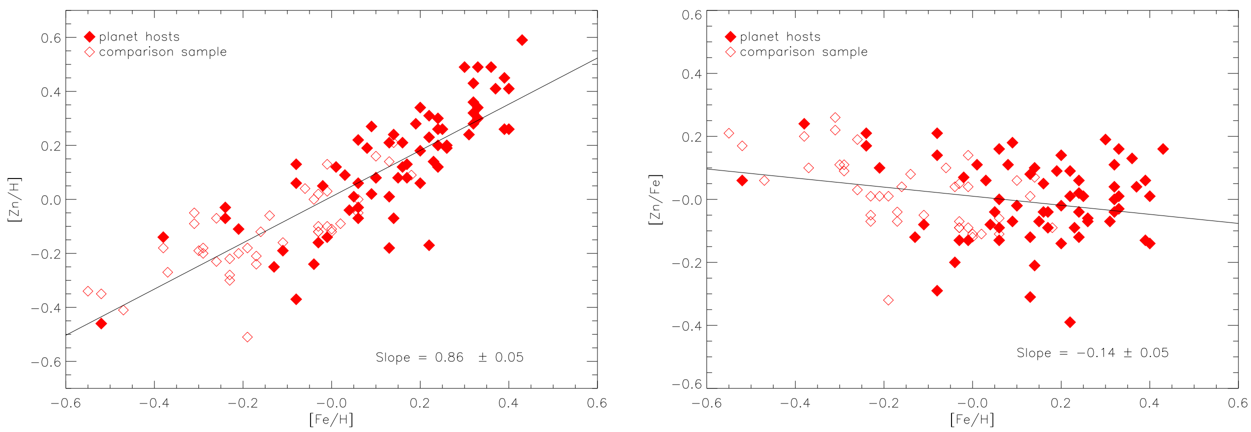

Fig. 10. [Zn/H] and [Zn/Fe] vs. [Fe/H] plots. Filled and open symbols represent planet host and comparison sample stars, respectively. Linear least-squares fits to both samples together are represented and slope values are indicated at the bottom of each plot.

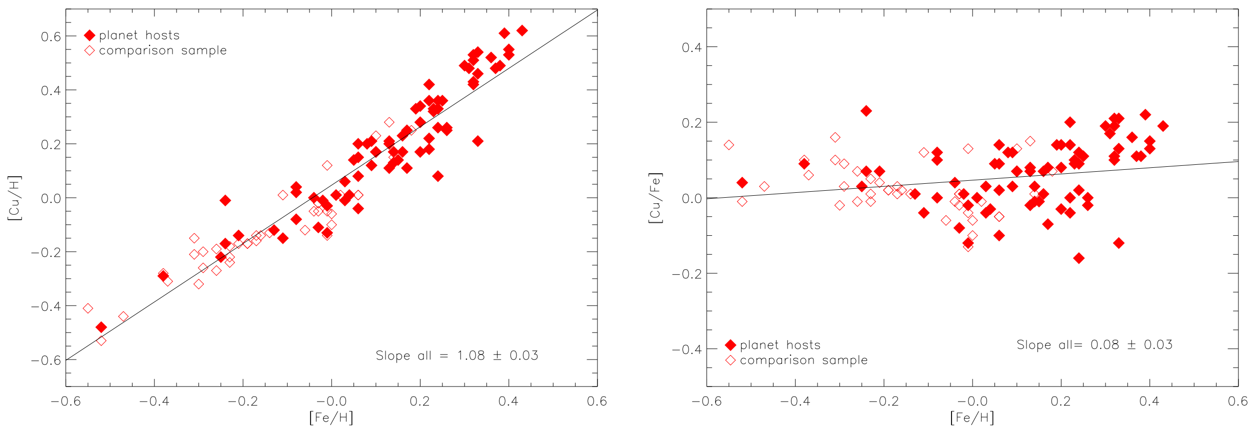

Fig. 11. [Cu/H] and [Cu/Fe] vs. [Fe/H] plots. Filled and open symbols represent planet host and comparison sample stars, respectively. Linear least-squares fits to both samples together are represented and slope values are indicated at the bottom of each plot.

EWs. Table **??** shows all the atmospheric parameters and the EW values for the 46 compared targets. All the measurements are in good agreement, especially for values of Gonzalez et al. (2001) from Keck spectra, with differences tipically lower than 2 mÅ. In some cases, our data differ from the values taken from Takeda et al. (2001), but the other sources agree better with our results (see HD 52265 and HD 89744). Only for HD 92788 is our measurement larger than the two values in the literature.

For sulphur, comparisons for 31 targets were possible. All the atmospheric parameters and S abundances are listed in Table **??**. [S/H] values from Santos et al. (2000) and Sadakane et al. (2002) are in good agreement with our results in most cases, with discrepancies lower than 0.2 dex. However, significant disagreements, of the order of 0.4 dex, appear when comparing with S abundances from Takeda et al. (2001). Using different lines and atomic parameters could be the cause of this discrepancy. Sadakane et al. (2002) synthesized the same S I lines as we did. Our results agree very well. Since Gonzalez et al. (2001) did not include a sensitivity study in their work, we could not scale their results to our atmospheric parameters, thus preventing a homogeneous comparison.

Zinc abundances were compared with literature values in nineteen targets (see Table **??**). We obtained similar results in almost all cases, with differences lower than 0.2 dex. Only HD 38529, HD 75732 and HD 145675 show clear discrepancies with results from Takeda et al. (2001). As for S, the cause of these differences could be that different methods, with different sets of lines, were used.

Sadakane et al. (2002) obtained copper abundances in eight planet host stars common to our work. The comparison is presented in Table **??**. The results are in very good agreement, with differences lower than 0.13 dex, except for HD 92788 and HD 134987. In these two cases, the results may diverge because of the different methods used. All the comparisons are represented in Fig. 13.

6. Discussion and conclusions

This article presents the abundances of one refractory (Cu) and three volatile (C, S and Zn) elements in a large set of planet-harbouring stars and in an unbiased volume-limited comparison sample of solar-type dwarfs with no known planetary mass companions. An independent and uniform study of the two

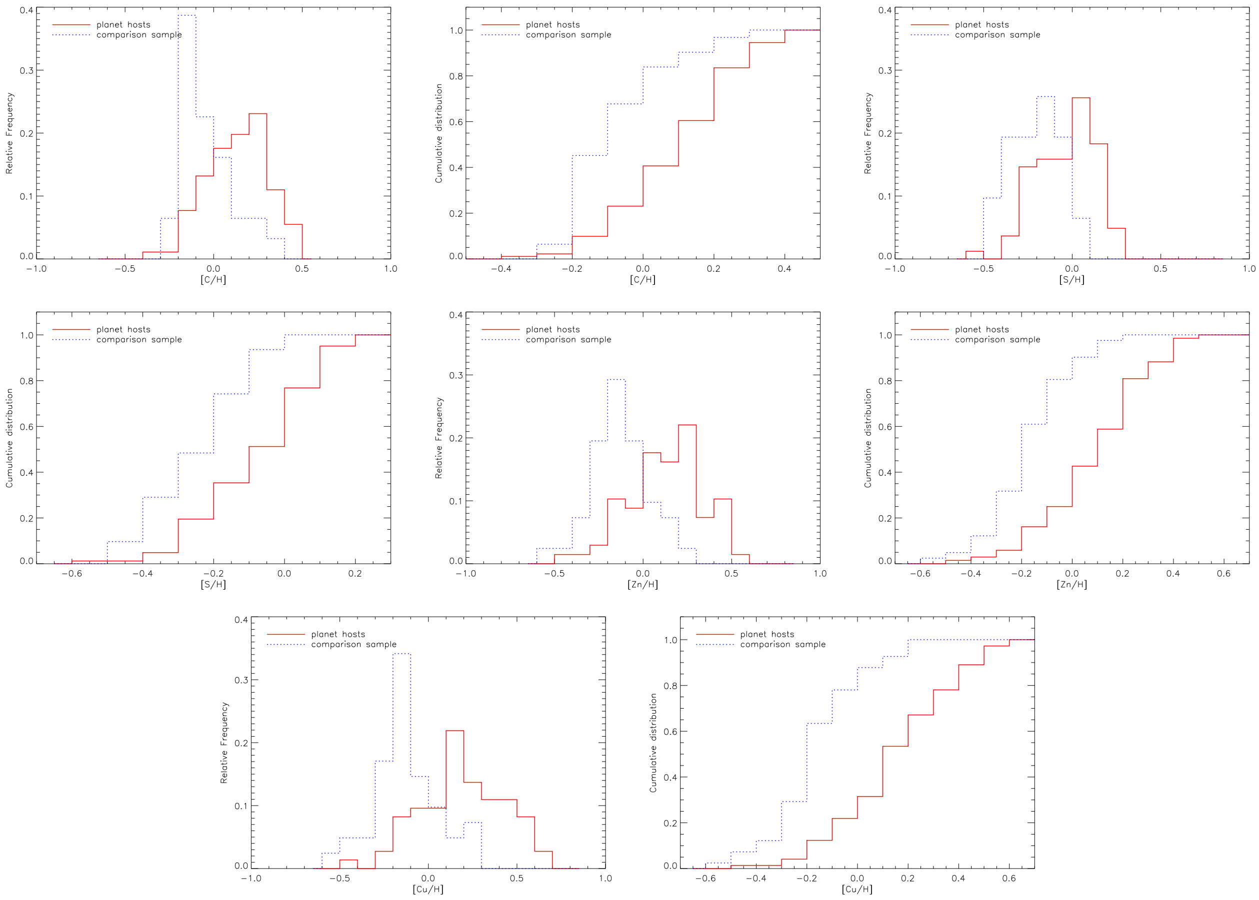

Fig. 12. [*X*/H] distributions for C, S, Zn and Cu. The solid and dotted lines represent planet host and comparison sample stars, respectively.

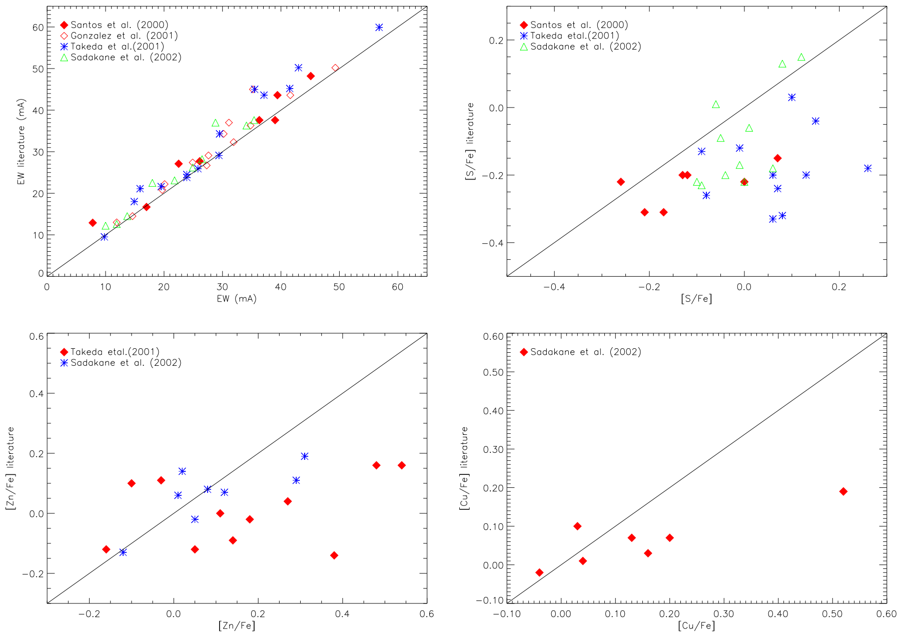

Fig. 13. *Top left*: comparison of the measured *EW*s of the C I line at 5380 Å with data given in Santos et al. (2000, filled diamonds), in Gonzalez et al. (2001, open diamonds), in Takeda et al. (2002, asterisks) and in Sadakane et al. (2002, triangles). *Top right*: comparison of [S/Fe] ratios from our work and from Santos et al. (2000, filled symbols), Takeda et al. (2002, asterisks) and Sadakane et al. (2002, triangles). *Bottom left*: comparison of [Zn/Fe] ratios from our work and from Takeda et al. (2002, filled diamonds) and Sadakane et al. (2002,asterisks).*Bottom right*: comparison of [Cu/Fe] ratios from our work and from Sadakane et al. (2002,filled diamonds).

Table 2. Atomic parameters adopted for C I, S I, Zn I and Cu I lines

Species	λ (Å)	χ_l (eV)	$\log gf$
C I	5380.340	7.68	−1.71
C I	5052.160	7.68	−1.42
S I	6743.440	7.87	−1.27
S I	6743.531	7.87	−0.92
S I	6743.640	7.87	−0.93
S I	6757.007	7.87	−0.81
S I	6757.177	7.87	−0.33
Zn I	4810.537	4.08	−0.13
Zn I	4722.160	4.03	−0.37
Cu I	5218.204	3.82	−1.33
Cu I	5218.206	3.82	−0.85
Cu I	5218.208	3.82	−0.98
Cu I	5218.210	3.82	−0.26
Cu I	5218.214	3.82	−0.48
Cu I	5218.216	3.82	−0.48
Cu I	5218.219	3.82	0.14
Cu I	5782.032	1.64	−3.53
Cu I	5782.042	1.64	−3.84
Cu I	5782.054	1.64	−3.14
Cu I	5782.064	1.64	−3.19
Cu I	5782.073	1.64	−3.49
Cu I	5782.084	1.64	−2.79
Cu I	5782.086	1.64	−3.14
Cu I	5782.098	1.64	−3.14
Cu I	5782.113	1.64	−2.79
Cu I	5782.124	1.64	−2.79
Cu I	5782.153	1.64	−2.69
Cu I	5782.173	1.64	−2.34

samples was performed for each element using atmospheric parameters derived from a detailed spectroscopic analysis by Santos et al. (2004a). We have carried out a careful comparison of our results with those already published by several authors and obtained a good agreement on the whole. The result is a significant study for the completeness and homogeneity of the four elements analysed.

Comparing trends and searching for differences between the two samples, stars with and without known planets, can provide clues toward clarifying the formation and evolution of planetary systems. In particular, the behaviour of volatile elements can be very informative for discriminating between the "self-enrichment" and the "primordial" hypotheses, and the relative importance of the differential accretion (Gonzalez 1997; Santos et al. 2000, 2001; Smith et al. 2001). If the accretion of large amounts of metal-rich rocky material were the principal reason for the observed enhancement in iron abundance in planet host stars, then volatiles would not show as much overabundance as refractories do in these targets.

Our results show that abundances of volatile elements have the same behaviour in stars with and without planets. The abundance trends for planet host and comparison sample stars are nearly indistinguishable. The planet host distributions are the natural extensions of the comparison sample trends toward high metallicities. This may imply that the accretion of rocky materials is not the principal cause of the metal-rich nature of stars with planets. Although the possibility of pollution is not excluded (see Laws & Gonzalez 2001; Israelian et al. 2001, 2003a), the hypothesis of a primordial metal-rich cloud out of which planetary systems would have formed seems likelier than the "self-enrichment" scenario, as an explanation for the observed metallicity enhancement.

Most of the evidence suggests a "primordial" origin for the metallicity excess (Pinsonneault et al. 2001; Santos et al. 2001, 2003b, 2004a). Previous studies of volatiles have already led to the same conclusion. Santos et al. (2000) found no significant differences in [C/Fe] and [O/Fe] trends between field stars from literature and eight planet host stars. Takeda et al. (2001) and Sadakane et al. (2002) arrived at the same conclusion by comparing refractory and volatile elements and searching for a T_C dependence. Ecuvillon et al. (2004) found that nitrogen abundances show the same behaviour in a large set of stars with and without known planets.

Furthermore, we have obtained negative slopes in the [X/Fe] trends for the three volatiles, while the [N/Fe] trend was previously found flat (Ecuvillon et al. 2004). Contrary to results obtained in previous studies (see Takeda et al. 2001; Sadakane et al. 2002), C, S and Zn abundances do not scale with that of iron. Since no differences are seen between the two samples, this behaviour must be evidence of the chemical evolution of the Galactic disc, with no link to the presence of planets. In fact, several studies of abundances in the Galactic disc have revealed just such a clear linear behaviour for carbon (Friel & Boesgaard 1992; Andersson & Edvardsson 1994; Gustafsson et al. 1999; Shi et al. 2002) and for sulphur (Takada-Hidai et al. 2002; Chen et al. 2002) in the metallicity range $-0.8 <$ [Fe/H] < 0.3. The [Zn/Fe] vs. [Fe/H] plot shows a decreasing trend for $-0.6 <$ [Fe/H] < 0 and a slight rise at metallicities above solar. A similar result has been recently obtained by Bensby et al. (2003) for 66 disc stars.

Concerning the refractory Cu, [Cu/Fe] vs. [Fe/H] plot reveals a behaviour similar to Zn, with a slight decrease at $-0.6 <$ [Fe/H] < 0 and a rise above the solar metallicity, steeper than for Zn. [Cu/Fe] is on average overabundant with respect to the solar value. The larger value of the slope resulting from fitting only stars with planets might be due to the observed [Cu/Fe] rise at [Fe/H] > 0, probably related to Galactic chemical evolutionary effects rather than to the presence of planets. In fact, planet host stars do not show different behaviour with respect to the comparison sample. Since all the available studies of Cu Galactic trends do not include the solar metallicity range, we cannot compare our results with those of the literature for this element.

The [X/Fe] trends must be compared with detailed models of Galactic chemical evolution to distinguish possible effects due to the presence of planets. In this framework, our work provides new additional data of C, S, Zn and Cu abundances to check Galactic chemical evolution models in the high [Fe/H] region. Because of the lack of detailed abundance studies reaching solar metallicities, our results can be very informative to improve our present understanding of stellar nucleosynthesis and chemical evolution.

In the future, it will be very important to manage uniform studies of other volatile and refractory elements, with a wide range of condensation temperatures T_C. Possible systematic trends of [X/H] in terms of T_C will give us conclusive information about the relative importance of differential accretion on the metallicity excess as a whole.

Acknowledgements. IRAF is distributed by the National Optical Astronomy Observatories, operated by the Association of Universities for Research in Astronomy, Inc., under contract with the National Science Foundation, USA.

References

Anders, E., & Grevesse, N. 1989, Geochim et. Cosmochim. Acta, 53, 197
Andersson, H., & Edvardsson, D. 1994, A&A, 290, 590
Bensby, T.,Feltzing, S., & Lundström, I. 2003, A&A, 410, 527
Bihain, G., Israelian, G., Rebolo, R., Bonifacio, P., & Molaro, P. 2004, A&A, submitted
Bodaghee, A., Santos, N. C., Israelian, G. & Mayor, M. 2003, A&A, 404, 715
Carretta, E., Gratton, R. G., & Sneden, C. 2000, A&A, 356, 238
Chen, Y. Q., Nissen, P. E., Zhao, G., & Apslund, M. 2002, A&A, 390, 225
Ecuvillon, A., Israelian, G., Santos, N.C., Mayor, M., R. J. García López, Randich, S., 2004, A&A, 418, 703
Edvardsson, B., Andersen, J., Gustafsson, B., Lambert, D. L., Nissen, P.E., & Tomkin, J. 1993, A&A, 275, 101
Friel, E. D., & Boesgaard, A. M. 1992, ApJ, 387, 170
Gonzalez, G. 1997, MNRAS, 285, 403
Gonzalez, G., & Laws, C. 2000, AJ, 119, 390
Gonzalez, G., Laws, C., Tyagi, S., & Reddy, B. E. 2001, AJ, 121, 432
Gurtovenko, E. A., & Kostyk, R. I. 1989, Fraunhoffer spectrum and system of solar oscillator strengths, KiIND, 200
Gustafsson, B., Karlsson, T., Olsson, E., Edvardsson, B., & Ryde, N. 1999, A&A, 342, 426
Israelian, G., Santos, N. C., Mayor, M., & Rebolo, R. 2001, Nature, 411, 163
Israelian, G., Santos, N. C., Mayor, M., & Rebolo, R. 2003a, A&A, 405, 753
Israelian, G. 2003b, in IAU S219: Stars as Suns: Activity, Evolution, and Planets, ed. A. K. Dupree (San Francisco: ASP), in press
Israelian, G., Santos, N. C., Mayor, M., & Rebolo, R. 2004, A&A, 414, 601
Kobulnicky, H. A., Skillman, E. D. 1998, ApJ, 497, 601
Kupka, F. G., Piskunov, N. E., Ryabchikova, T. A., Stempels, H. C., Weiss, W. W., 1999, A&AS, 138, 119
Kurucz, R. L. 1993, CD-ROMs, ATLAS9 Stellar Atmospheres Programs and 2 km s^{-1} Grid (Cambridge: Smithsonian Astrophys. Obs.)
Kurucz, R. L., Furenlid, I., Brault, J., Testerman, L. 1984, Solar Flux Atlas from 296 to 1300 nm, NOAO Atlas No. 1
Laws, C. & Gonzalez, G. 2001, ApJ, 553, 405
Laws, C., Gonzalez, G., Walker, K. M., Tyagi, S., Dodsworth, J., Snider, K. & Suntzeff, N. 2003, AJ, 125, 2664
Luck, R. E., & Bond, H. E. 1985, ApJ, 292, 559
Mayor, M. & Queloz, D. 1995, Nature, 378, 355
Mishenina, T. V., Kovtyukh, V. V., Soubiran, C., Travaglio, C., Busso, M., 2002, A&A, 396, 189
Murray, N., & Chaboyer, B. 2002, ApJ, 566, 442
Pinsonneault, M. H., DePoy, D. L., & Coffee, M., 2001, ApJ, 556, L59
Prantzos, N., Vangioni-Flam E., Chauveau, S. 1994, A&A, 285, 132
Reid, I. N. 2002, PASP, 114, 306
Sadakane, K., Ohkubo, Y., Takeda, Y., Sato, B., Kambe, E., & Aoki, W. 2002, PASJ, 54, 911
Sandquist, E. L., Dokter, J. J., Lin, D. N. C., & Mardling, R. 2002, ApJ, 572, 1012
Santos, N. C., Israelian, G., & Mayor, M. 2000, A&A 363, 228
Santos, N. C., Israelian, G., & Mayor, M. 2001, A&A 373, 1019
Santos, N. C., García López, R. J., Israelian, G., Mayor, M., Rebolo, R., García-Gil, A., Pérez de Taoro, M. R., & Randich, S. 2002, A&A, 386, 1028
Santos, N. C., Mayor, M., Udry, S., et al., 2003a, in IAU S219: Stars as Suns: Activity, Evolution, and Planets, ed. A. K. Dupree (San Francisco: ASP), in press
Santos, N. C., Israelian, G., Mayor, M., Rebolo, R., & Udry, S. 2003b, A&A,398,363
Santos, N. C., Israelian, G., & Mayor, M. 2004a, A&A, 415, 1153
Santos, N.C., Israelian, G., García López, R. J., Mayor, M., Rebolo, R., Randich, S., Ecuvillon, A., & Cerdeña, C. 2004b, A&A, submitted
Shi, J. R., Zhao, G., & Chen, Y. Q. 2002, A&A, 381, 982
Smith, V. V., Cunha, K., & Lazzaro, D., 2001, AJ, 121,3207
Sneden, C. 1973, Ph.D. thesis, University of Texas
Sneden, C., Gratton, R. G., Crocker, D. A. 1991, A&A, 246, 354
Steffen, M. 1985, A&AS, 59, 403
Takada-Hidai, M., Takeda, Y., Sato, S., Honda, S., Sadakane, K., Kawanomoto, S., Sargent, W. L. W., Lu, L., & Barlow, T. 2002, ApJ, 573, 614
Takeda, Y., Sato, B., Kambe, E., Aoki, W., Honda, S., Kawanomoto, S., & Masuda, S., et al. 2001, PASJ, 53, 1211
Thévenin, F. & Idiart, T. P. 1999, ApJ, 521, 753
Timmes, F. X., Woosley, S. E., & Weaver, T. A. 1995, ApJS, 98, 617
Vauclair, S. 2003, ApJ, to be published in ApJ, April 20

Table 4: Carbon abundances from CI lines at 5380 Å and 5052 Å for a set of stars with planets and brown dwarf companions

Star	$T_{\rm eff}$ (K)	$\log g$ (cm s^{-2})	ξ_t (km s^{-1})	[Fe/H]	EW$_{5380}$ (mÅ)	EW$_{5052}$ (mÅ)	[C/Fe]
HD 142	6302 ± 56	4.34 ± 0.13	1.86 ± 0.17	0.14 ± 0.07	52.1	69.1	0.10 ± 0.08
HD 1237	5536 ± 50	4.56 ± 0.12	1.33 ± 0.06	0.12 ± 0.06	16.7	27.6	−0.06 ± 0.05
HD 2039	5976 ± 51	4.45 ± 0.10	1.26 ± 0.07	0.32 ± 0.06	33.3	52.8	−0.13 ± 0.05
HD 3651	5173 ± 35	4.37 ± 0.12	0.74 ± 0.05	0.12 ± 0.04	12.9	20.1	−0.01 ± 0.07
HD 4203	5636 ± 40	4.23 ± 0.14	1.12 ± 0.05	0.40 ± 0.05	41.0	55.9	0.05 ± 0.07
HD 4208	5626 ± 32	4.49 ± 0.10	0.95 ± 0.06	−0.24 ± 0.04	20.5	22.2	0.23 ± 0.19
HD 6434	5835 ± 59	4.60 ± 0.12	1.53 ± 0.27	−0.52 ± 0.08	19.0	21.0	0.40 ± 0.19
HD 8574	6151 ± 57	4.51 ± 0.10	1.45 ± 0.15	0.06 ± 0.07	33.4	45.4	−0.01 ± 0.09
HD 9826	6212 ± 64	4.26 ± 0.13	1.69 ± 0.16	0.13 ± 0.08	47.8	64.6	0.07 ± 0.07
HD 10647	6130 ± 31	4.48 ± 0.08	1.40 ± 0.08	−0.03 ± 0.04	27.2	41.2	−0.01 ± 0.04
HD 10697	5641 ± 28	4.05 ± 0.05	1.13 ± 0.03	0.14 ± 0.04	27.4	43.2	−0.01 ± 0.03
HD 12661	5702 ± 36	4.33 ± 0.08	1.05 ± 0.04	0.36 ± 0.05	32.3	52.2	−0.05 ± 0.05
HD 13445	5163 ± 00	4.52 ± 0.00	0.72 ± 0.00	−0.24 ± 0.00	12.9	12.7	0.31 ± 0.24
HD 16141	5801 ± 30	4.22 ± 0.12	1.34 ± 0.04	0.15 ± 0.04	28.2	41.2	−0.08 ± 0.06
HD 17051	6252 ± 53	4.61 ± 0.16	1.18 ± 0.10	0.26 ± 0.06	47.7	61.4	0.02 ± 0.10
HD 19994	6190 ± 00	4.19 ± 0.00	1.54 ± 0.00	0.24 ± 0.00	61.6	74.9	0.15 ± 0.09
HD 20367	6138 ± 79	4.53 ± 0.22	1.22 ± 0.16	0.17 ± 0.10	23.2	39.6	−0.28 ± 0.09
HD 22049	5073 ± 42	4.43 ± 0.08	1.05 ± 0.06	−0.13 ± 0.05	9.9	14.5	0.19 ± 0.10
HD 23079	5959 ± 46	4.35 ± 0.12	1.20 ± 0.10	−0.11 ± 0.06	23.1	36.3	0.03 ± 0.06
HD 23596	6108 ± 36	4.25 ± 0.10	1.30 ± 0.05	0.31 ± 0.05	44.5	65.7	−0.05 ± 0.04
HD 27442	4825 ± 107	3.55 ± 0.32	1.18 ± 0.12	0.39 ± 0.13	16.8	26.0	−0.05 ± 0.13
HD 28185	5656 ± 44	4.45 ± 0.08	1.01 ± 0.06	0.22 ± 0.05	27.8	42.4	0.03 ± 0.05
HD 30177	5587 ± 00	4.29 ± 0.00	1.08 ± 0.00	0.38 ± 0.00	37.6	54.6	0.08 ± 0.02
HD 33636	6046 ± 49	4.71 ± 0.09	1.79 ± 0.19	−0.08 ± 0.06	24.4	32.7	0.28 ± 0.11
HD 37124	5546 ± 30	4.50 ± 0.03	0.80 ± 0.07	−0.38 ± 0.04	13.0	19.9	0.29 ± 0.06
HD 38529	5674 ± 40	3.94 ± 0.12	1.38 ± 0.05	0.40 ± 0.06	45.0	53.3	−0.06 ± 0.14
HD 39091	5991 ± 27	4.42 ± 0.10	1.24 ± 0.04	0.10 ± 0.04	30.7	43.8	−0.03 ± 0.06
HD 40979	6145 ± 42	4.31 ± 0.15	1.29 ± 0.09	0.21 ± 0.05	34.7	55.8	−0.11 ± 0.07
HD 46375	5268 ± 55	4.41 ± 0.16	0.97 ± 0.06	0.20 ± 0.06	20.8	27.0	0.08 ± 0.14
HD 49674	5644 ± 54	4.37 ± 0.07	0.89 ± 0.07	0.33 ± 0.06	25.9	34.9	−0.19 ± 0.09
HD 50554	6026 ± 30	4.41 ± 0.13	1.11 ± 0.06	0.01 ± 0.04	28.3	40.7	−0.00 ± 0.07
HD 52265	6105 ± 00	4.28 ± 0.00	1.36 ± 0.00	0.23 ± 0.00	43.6	66.9	0.04 ± 0.03
HD 65216	5666 ± 31	4.53 ± 0.09	1.06 ± 0.05	−0.12 ± 0.04	12.3	21.4	−0.07 ± 0.04
HD 68988	5988 ± 52	4.45 ± 0.15	1.25 ± 0.08	0.36 ± 0.06	35.7	-	−0.14 ± 0.06
HD 72659	5995 ± 45	4.30 ± 0.07	1.42 ± 0.09	0.03 ± 0.06	23.4	36.7	−0.14 ± 0.04
HD 73256	5518 ± 49	4.42 ± 0.12	1.22 ± 0.06	0.26 ± 0.06	24.8	30.6	−0.08 ± 0.14
HD 73526	5699 ± 49	4.27 ± 0.12	1.26 ± 0.06	0.27 ± 0.06	28.7	43.2	−0.10 ± 0.06
HD 74156	6112 ± 39	4.34 ± 0.10	1.38 ± 0.07	0.16 ± 0.05	39.1	54.9	−0.00 ± 0.06
HD 75289	6143 ± 53	4.42 ± 0.13	1.53 ± 0.09	0.28 ± 0.07	37.6	56.6	−0.13 ± 0.06
HD 75732	5279 ± 62	4.37 ± 0.18	0.98 ± 0.07	0.33 ± 0.07	21.6	29.6	−0.02 ± 0.12
HD 76700	5737 ± 34	4.25 ± 0.14	1.18 ± 0.04	0.41 ± 0.05	32.3	46.1	−0.20 ± 0.07
HD 80606	5574 ± 72	4.46 ± 0.20	1.14 ± 0.09	0.32 ± 0.09	25.2	42.4	−0.04 ± 0.09
HD 82943	6015 ± 00	4.46 ± 0.00	1.13 ± 0.00	0.30 ± 0.00	37.6	66.8	0.02 ± 0.11
HD 83443	5454 ± 61	4.33 ± 0.17	1.08 ± 0.08	0.35 ± 0.08	27.7	41.0	−0.00 ± 0.08
HD 89744	6234 ± 45	3.98 ± 0.05	1.62 ± 0.08	0.22 ± 0.05	51.4	75.1	0.03 ± 0.04
HD 92788	5821 ± 41	4.45 ± 0.06	1.16 ± 0.05	0.32 ± 0.05	37.0	47.2	−0.05 ± 0.11
HD 95128	5954 ± 25	4.44 ± 0.10	1.30 ± 0.04	0.06 ± 0.03	25.9	42.5	−0.03 ± 0.04
HD 106252	5899 ± 35	4.34 ± 0.07	1.08 ± 0.06	−0.01 ± 0.05	23.1	37.0	−0.04 ± 0.03
HD 108147	6248 ± 42	4.49 ± 0.16	1.35 ± 0.08	0.20 ± 0.05	37.5	56.5	−0.07 ± 0.06
HD 108874	5596 ± 42	4.37 ± 0.12	0.89 ± 0.05	0.23 ± 0.05	27.5	36.3	−0.02 ± 0.10
HD 111232	5494 ± 26	4.50 ± 0.10	0.84 ± 0.05	−0.36 ± 0.04	10.2	16.1	0.17 ± 0.06
HD 114729	5886 ± 36	4.28 ± 0.13	1.25 ± 0.09	−0.25 ± 0.05	16.2	32.8	0.05 ± 0.10

Table 4: Continued.

Star	$T_{\rm eff}$ (K)	$\log g$ (cm s^{-2})	ξ_t (km s^{-1})	[Fe/H]	EW$_{5380}$ (mÅ)	EW$_{5052}$ (mÅ)	[C/Fe]
HD 114762	5884 ± 34	4.22 ± 0.02	1.31 ± 0.17	−0.70 ± 0.04	12.2	21.2	0.33 ± 0.03
HD 114783	5098 ± 36	4.45 ± 0.11	0.74 ± 0.05	0.09 ± 0.04	17.2	22.6	0.24 ± 0.13
HD 117176	5560 ± 34	4.07 ± 0.05	1.18 ± 0.05	−0.06 ± 0.05	18.0	29.4	−0.01 ± 0.03
HD 120136	6339 ± 73	4.19 ± 0.10	1.70 ± 0.16	0.23 ± 0.07	59.9	85.1	0.19 ± 0.08
HD 121504	6075 ± 40	4.64 ± 0.12	1.31 ± 0.07	0.16 ± 0.05	29.7	41.8	−0.10 ± 0.08
HD 130322	5392 ± 36	4.48 ± 0.06	0.85 ± 0.05	0.03 ± 0.04	14.5	19.5	−0.03 ± 0.11
HD 134987	5776 ± 29	4.36 ± 0.07	1.09 ± 0.04	0.30 ± 0.04	36.3	55.2	0.03 ± 0.03
HD 136118	6222 ± 39	4.27 ± 0.15	1.79 ± 0.12	−0.04 ± 0.05	36.9	53.4	0.07 ± 0.06
HD 137759	4775 ± 113	3.09 ± 0.40	1.78 ± 0.11	0.13 ± 0.14	17.3	25.5	0.08 ± 0.16
HD 141937	5909 ± 39	4.51 ± 0.08	1.13 ± 0.06	0.10 ± 0.05	28.2	49.4	0.07 ± 0.06
HD 142415	6045 ± 44	4.53 ± 0.08	1.12 ± 0.07	0.21 ± 0.05	24.5	41.0	−0.23 ± 0.05
HD 143761	5853 ± 25	4.41 ± 0.15	1.35 ± 0.07	−0.21 ± 0.04	21.1	33.5	0.16 ± 0.05
HD 145675	5311 ± 87	4.42 ± 0.18	0.92 ± 0.10	0.43 ± 0.08	24.5	34.4	−0.01 ± 0.11
HD 147513	5883 ± 25	4.51 ± 0.05	1.18 ± 0.04	0.06 ± 0.04	22.0	32.5	−0.11 ± 0.06
HD 150706	5961 ± 27	4.50 ± 0.10	1.11 ± 0.06	−0.01 ± 0.04	19.1	30.3	−0.13 ± 0.04
HD 160691	5798 ± 33	4.31 ± 0.08	1.19 ± 0.04	0.32 ± 0.04	35.2	54.2	−0.04 ± 0.04
HD 168443	5617 ± 35	4.22 ± 0.05	1.21 ± 0.05	0.06 ± 0.05	26.7	42.3	0.13 ± 0.03
HD 168746	5601 ± 33	4.41 ± 0.12	0.99 ± 0.05	−0.08 ± 0.05	22.5	29.3	0.17 ± 0.12
HD 169830	6299 ± 41	4.10 ± 0.02	1.42 ± 0.09	0.21 ± 0.05	48.2	70.5	−0.02 ± 0.04
HD 177830	4804 ± 77	3.57 ± 0.17	1.14 ± 0.09	0.33 ± 0.09	23.9	25.0	0.15 ± 0.24
HD 178911B	5600 ± 42	4.44 ± 0.08	0.95 ± 0.05	0.27 ± 0.05	23.0	39.0	−0.08 ± 0.05
HD 179949	6260 ± 43	4.43 ± 0.05	1.41 ± 0.09	0.22 ± 0.05	40.5	70.6	0.00 ± 0.11
HD 186427	5772 ± 25	4.40 ± 0.07	1.07 ± 0.04	0.08 ± 0.04	23.8	37.0	−0.03 ± 0.03
HD 187123	5845 ± 22	4.42 ± 0.07	1.10 ± 0.03	0.13 ± 0.03	26.2	39.1	−0.07 ± 0.04
HD 190228	5325 ± 00	3.90 ± 0.00	1.11 ± 0.00	−0.26 ± 0.00	12.6	18.4	0.07 ± 0.07
HD 190360	5584 ± 36	4.37 ± 0.06	1.07 ± 0.05	0.24 ± 0.05	30.5	41.0	0.05 ± 0.09
HD 195019	5859 ± 31	4.32 ± 0.07	1.27 ± 0.05	0.09 ± 0.04	29.0	39.8	−0.03 ± 0.07
HD 196050	5918 ± 44	4.35 ± 0.13	1.39 ± 0.06	0.22 ± 0.05	38.5	66.3	0.11 ± 0.10
HD 202206	5752 ± 53	4.50 ± 0.09	1.01 ± 0.06	0.35 ± 0.06	27.1	37.6	−0.21 ± 0.08
HD 210277	5532 ± 00	4.29 ± 0.00	1.03 ± 0.00	0.19 ± 0.00	27.7	38.2	0.05 ± 0.07
HD 213240	5984 ± 33	4.25 ± 0.10	1.25 ± 0.05	0.17 ± 0.05	36.1	55.5	−0.00 ± 0.04
HD 216435	5938 ± 42	4.12 ± 0.05	1.28 ± 0.06	0.24 ± 0.05	46.5	63.0	0.07 ± 0.05
HD 216437	5887 ± 32	4.30 ± 0.07	1.31 ± 0.04	0.25 ± 0.04	37.0	55.9	0.01 ± 0.03
HD 216770	5423 ± 41	4.40 ± 0.13	1.01 ± 0.05	0.26 ± 0.04	20.0	28.2	−0.11 ± 0.09
HD 217014	5804 ± 36	4.42 ± 0.07	1.20 ± 0.05	0.20 ± 0.05	34.3	48.2	0.05 ± 0.06
HD 217107	5645 ± 00	4.31 ± 0.00	1.06 ± 0.00	0.37 ± 0.00	29.3	44.0	−0.13 ± 0.02
HD 219542B	5732 ± 31	4.40 ± 0.05	0.99 ± 0.04	0.17 ± 0.04	19.8	29.2	−0.23 ± 0.06
HD 222404	4916 ± 70	3.36 ± 0.21	1.27 ± 0.06	0.16 ± 0.08	12.6	20.7	−0.19 ± 0.09
HD 222582	5843 ± 38	4.45 ± 0.07	1.03 ± 0.06	0.05 ± 0.05	22.2	38.8	−0.03 ± 0.05

Table 5: Carbon abundances from CI lines at 5380 Å and 5052 Å for a set of comparison stars.

Star	$T_{\rm eff}$ (K)	$\log g$ (cm s^{-2})	ξ_t (km s^{-1})	[Fe/H]	EW$_{5380}$ (mÅ)	EW$_{5052}$ (mÅ)	[C/Fe]
HD 1581	5956 ± 44	4.39 ± 0.13	1.07 ± 0.09	−0.14 ± 0.05	18.8	30.7	−0.04 ± 0.05
HD 4391	5878 ± 53	4.74 ± 0.15	1.13 ± 0.10	−0.03 ± 0.06	18.9	35.8	0.07 ± 0.08
HD 7570	6140 ± 41	4.39 ± 0.16	1.50 ± 0.08	0.18 ± 0.05	39.9	62.2	0.03 ± 0.07
HD 10700	5344 ± 29	4.57 ± 0.09	0.91 ± 0.06	−0.52 ± 0.04	7.0	12.6	0.33 ± 0.04
HD 14412	5368 ± 24	4.55 ± 0.05	0.88 ± 0.05	−0.47 ± 0.03	7.5	10.2	0.22 ± 0.12
HD 17925	5180 ± 56	4.44 ± 0.13	1.33 ± 0.08	0.06 ± 0.07	9.2	15.6	−0.10 ± 0.07
HD 20010	6275 ± 57	4.40 ± 0.37	2.41 ± 0.41	−0.19 ± 0.07	29.1	45.0	0.08 ± 0.13

Table 5: Continued.

Star	$T_{\rm eff}$ (K)	$\log g$ (cm s^{-2})	ξ_t (km s^{-1})	[Fe/H]	EW$_{5380}$ (mÅ)	EW$_{5052}$ (mÅ)	[C/Fe]
HD 20766	5733 ± 31	4.55 ± 0.10	1.09 ± 0.06	−0.21 ± 0.04	14.0	26.3	0.10 ± 0.05
HD 20794	5444 ± 31	4.47 ± 0.07	0.98 ± 0.06	−0.38 ± 0.04	10.1	18.0	0.25 ± 0.03
HD 20807	5843 ± 26	4.47 ± 0.10	1.17 ± 0.06	−0.23 ± 0.04	16.2	30.4	0.11 ± 0.06
HD 23249	5074 ± 60	3.77 ± 0.16	1.08 ± 0.06	0.13 ± 0.08	17.0	30.2	0.07 ± 0.08
HD 23484	5176 ± 45	4.41 ± 0.17	1.03 ± 0.06	0.06 ± 0.05	8.5	12.7	−0.19 ± 0.10
HD 26965	5126 ± 34	4.51 ± 0.08	0.60 ± 0.07	−0.31 ± 0.04	11.5	14.4	0.42 ± 0.15
HD 30495	5868 ± 30	4.55 ± 0.10	1.24 ± 0.05	0.02 ± 0.04	18.4	31.6	−0.10 ± 0.04
HD 36435	5479 ± 37	4.61 ± 0.07	1.12 ± 0.05	0.00 ± 0.05	11.6	25.0	−0.01 ± 0.09
HD 38858	5752 ± 32	4.53 ± 0.07	1.26 ± 0.07	−0.23 ± 0.05	12.1	24.4	0.02 ± 0.07
HD 43162	5633 ± 35	4.48 ± 0.07	1.24 ± 0.05	−0.01 ± 0.04	13.8	24.0	−0.12 ± 0.03
HD 43834	5594 ± 36	4.41 ± 0.09	1.05 ± 0.04	0.10 ± 0.05	21.1	32.2	−0.01 ± 0.06
HD 53705	5825 ± 20	4.37 ± 0.10	1.20 ± 0.04	−0.19 ± 0.03	19.3	33.1	0.12 ± 0.04
HD 53706	5260 ± 31	4.35 ± 0.11	0.74 ± 0.05	−0.26 ± 0.04	11.0	14.8	0.18 ± 0.13
HD 65907	5979 ± 31	4.59 ± 0.12	1.36 ± 0.10	−0.29 ± 0.04	21.0	35.6	0.25 ± 0.05
HD 69830	5410 ± 26	4.38 ± 0.07	0.89 ± 0.03	−0.03 ± 0.04	14.2	24.2	0.05 ± 0.03
HD 72673	5242 ± 28	4.50 ± 0.09	0.69 ± 0.05	−0.37 ± 0.04	8.5	17.4	0.35 ± 0.05
HD 74576	5000 ± 55	4.55 ± 0.13	1.07 ± 0.08	−0.03 ± 0.06	13.7	20.9	0.40 ± 0.09
HD 76151	5803 ± 29	4.50 ± 0.08	1.02 ± 0.04	0.14 ± 0.04	23.3	38.5	−0.07 ± 0.03
HD 84117	6167 ± 37	4.35 ± 0.10	1.42 ± 0.09	−0.03 ± 0.05	33.7	50.9	0.07 ± 0.04
HD 189567	5765 ± 24	4.52 ± 0.05	1.22 ± 0.05	−0.23 ± 0.04	17.5	25.7	0.13 ± 0.06
HD 192310	5069 ± 49	4.38 ± 0.19	0.79 ± 0.07	−0.01 ± 0.05	16.7	18.6	0.28 ± 0.21
HD 196761	5435 ± 39	4.48 ± 0.08	0.91 ± 0.07	−0.29 ± 0.05	11.5	15.8	0.15 ± 0.12
HD 207129	5910 ± 24	4.42 ± 0.05	1.14 ± 0.04	0.00 ± 0.04	19.9	34.1	−0.10 ± 0.03
HD 211415	5890 ± 30	4.51 ± 0.07	1.12 ± 0.07	−0.17 ± 0.04	18.4	30.4	0.07 ± 0.03

Table 6: Sulphur abundances from SI lines at 6743 Å and 6757 Å for a set of stars with planets and brown dwarf companions.

Star	$T_{\rm eff}$ (K)	$\log g$ (cm s^{-2})	ξ_t (km s^{-1})	[Fe/H]	[S/Fe]$_1$	[S/Fe]$_2$	[S/Fe]
HD 142	6302 ± 56	4.34 ± 0.13	1.86 ± 0.17	0.14 ± 0.07	–	−0.39	−0.39 ± 0.09
HD 1237	5536 ± 50	4.56 ± 0.12	1.33 ± 0.06	0.12 ± 0.06	–	−0.22	−0.22 ± 0.08
HD 2039	5976 ± 51	4.45 ± 0.10	1.26 ± 0.07	0.32 ± 0.06	–	−0.17	−0.17 ± 0.08
HD 3651	5173 ± 35	4.37 ± 0.12	0.74 ± 0.05	0.12 ± 0.04	0.13	0.08	0.11 ± 0.08
HD 4203	5636 ± 40	4.23 ± 0.14	1.12 ± 0.05	0.40 ± 0.05	−0.20	−0.20	−0.20 ± 0.08
HD 4208	5626 ± 32	4.49 ± 0.10	0.95 ± 0.06	−0.24 ± 0.04	−0.16	−0.11	−0.14 ± 0.07
HD 6434	5835 ± 59	4.60 ± 0.12	1.53 ± 0.27	−0.52 ± 0.08	–	−0.18	−0.18 ± 0.09
HD 8574	6151 ± 57	4.51 ± 0.10	1.45 ± 0.15	0.06 ± 0.07	−0.11	−0.11	−0.11 ± 0.08
HD 9826	6212 ± 64	4.26 ± 0.13	1.69 ± 0.16	0.13 ± 0.08	−0.33	–	−0.33 ± 0.09
HD 10647	6143 ± 31	4.48 ± 0.08	1.40 ± 0.08	−0.03 ± 0.04	−0.12	−0.12	−0.12 ± 0.06
HD 10697	5641 ± 28	4.05 ± 0.05	1.13 ± 0.03	0.14 ± 0.04	−0.19	–	−0.19 ± 0.06
HD 12661	5702 ± 36	4.33 ± 0.08	1.05 ± 0.04	0.36 ± 0.05	−0.26	−0.26	−0.26 ± 0.07
HD 13445	5163 ± 00	4.52 ± 0.00	0.72 ± 0.00	−0.24 ± 0.00	0.04	−0.06	−0.01 ± 0.07
HD 16141	5801 ± 30	4.22 ± 0.12	1.34 ± 0.04	0.15 ± 0.04	−0.10	−0.15	−0.12 ± 0.08
HD 17051	6252 ± 53	4.61 ± 0.16	1.18 ± 0.10	0.26 ± 0.06	−0.26	−0.26	−0.26 ± 0.09
HD 19994	6190 ± 00	4.19 ± 0.00	1.54 ± 0.00	0.24 ± 0.00	−0.29	−0.29	−0.29 ± 0.05
HD 22049	5073 ± 42	4.43 ± 0.08	1.05 ± 0.06	−0.13 ± 0.05	−0.02	0.03	0.00 ± 0.08
HD 23079	5959 ± 46	4.35 ± 0.12	1.20 ± 0.10	−0.11 ± 0.06	−0.24	−0.24	−0.24 ± 0.08
HD 23596	6108 ± 36	4.25 ± 0.10	1.30 ± 0.05	0.31 ± 0.05	−0.26	−0.21	−0.23 ± 0.08
HD 28185	5656 ± 44	4.45 ± 0.08	1.01 ± 0.06	0.22 ± 0.05	−0.12	−0.07	−0.09 ± 0.08
HD 30177	5587 ± 00	4.29 ± 0.00	1.08 ± 0.00	0.38 ± 0.00	–	−0.23	−0.23 ± 0.05
HD 33636	6046 ± 49	4.71 ± 0.09	1.79 ± 0.19	−0.08 ± 0.06	−0.12	−0.12	−0.12 ± 0.08

Table 6: Continued.

Star	$T_{\rm eff}$ (K)	$\log g$ (cm s^{-2})	ξ_t (km s^{-1})	[Fe/H]	[S/Fe]$_1$	[S/Fe]$_2$	[S/Fe]
HD 37124	5546 ± 30	4.50 ± 0.03	0.80 ± 0.07	−0.38 ± 0.04	0.13	0.18	0.16 ± 0.07
HD 38529	5674 ± 40	3.94 ± 0.12	1.38 ± 0.05	0.40 ± 0.06	−0.35	−0.30	−0.33 ± 0.08
HD 39091	5991 ± 27	4.42 ± 0.10	1.24 ± 0.04	0.10 ± 0.04	−0.15	−0.20	−0.18 ± 0.07
HD 40979	6145 ± 42	4.31 ± 0.15	1.29 ± 0.09	0.21 ± 0.05	−0.21	−0.21	−0.21 ± 0.08
HD 46375	5268 ± 55	4.41 ± 0.16	0.97 ± 0.06	0.20 ± 0.06	0.05	0.00	0.03 ± 0.10
HD 47536	4554 ± 85	2.48 ± 0.23	1.82 ± 0.08	−0.54 ± 0.12	0.29	0.24	0.26 ± 0.13
HD 49674	5644 ± 54	4.37 ± 0.07	0.89 ± 0.07	0.33 ± 0.06	−0.23	−0.18	−0.20 ± 0.08
HD 50554	6026 ± 30	4.41 ± 0.13	1.11 ± 0.06	0.01 ± 0.04	−0.31	−0.36	−0.34 ± 0.08
HD 52265	6105 ± 00	4.28 ± 0.00	1.36 ± 0.00	0.23 ± 0.00	−0.23	−0.18	−0.21 ± 0.06
HD 65216	5666 ± 31	4.53 ± 0.09	1.06 ± 0.05	−0.12 ± 0.04	−0.03	−0.03	−0.03 ± 0.07
HD 68988	5988 ± 52	4.45 ± 0.15	1.25 ± 0.08	0.36 ± 0.06	−0.21	−0.16	−0.19 ± 0.09
HD 72659	5995 ± 45	4.30 ± 0.07	1.42 ± 0.09	0.03 ± 0.06	−0.28	−0.23	−0.26 ± 0.08
HD 73256	5518 ± 49	4.42 ± 0.12	1.22 ± 0.06	0.26 ± 0.06	−0.21	−0.26	−0.24 ± 0.09
HD 73526	5699 ± 49	4.27 ± 0.12	1.26 ± 0.06	0.27 ± 0.06	−0.27	−0.17	−0.22 ± 0.09
HD 74156	6112 ± 39	4.34 ± 0.10	1.38 ± 0.07	0.16 ± 0.05	−0.31	−0.26	−0.29 ± 0.08
HD 75289	6143 ± 53	4.42 ± 0.13	1.53 ± 0.09	0.28 ± 0.07	−0.33	−0.28	−0.31 ± 0.09
HD 75732	5279 ± 62	4.37 ± 0.18	0.98 ± 0.07	0.33 ± 0.07	−0.23	−0.18	−0.21 ± 0.10
HD 76700	5737 ± 34	4.25 ± 0.14	1.18 ± 0.04	0.41 ± 0.05	−0.31	−0.31	−0.31 ± 0.08
HD 80606	5574 ± 72	4.46 ± 0.20	1.14 ± 0.09	0.32 ± 0.09	−0.22	−0.22	−0.22 ± 0.11
HD 82943	6015 ± 00	4.46 ± 0.00	1.13 ± 0.00	0.30 ± 0.00	−0.20	−0.20	−0.20 ± 0.05
HD 83443	5454 ± 61	4.33 ± 0.17	1.08 ± 0.08	0.35 ± 0.08	–	−0.15	−0.15 ± 0.10
HD 92788	5821 ± 41	4.45 ± 0.06	1.16 ± 0.05	0.32 ± 0.05	–	−0.22	−0.22 ± 0.07
HD 95128	5954 ± 25	4.44 ± 0.10	1.30 ± 0.04	0.06 ± 0.03	−0.16	−0.16	−0.16 ± 0.06
HD 106252	5899 ± 35	4.34 ± 0.07	1.08 ± 0.06	−0.01 ± 0.05	–	−0.09	−0.09 ± 0.07
HD 108147	6248 ± 42	4.49 ± 0.16	1.35 ± 0.08	0.20 ± 0.05	−0.25	−0.25	−0.25 ± 0.08
HD 111232	5494 ± 26	4.50 ± 0.10	0.84 ± 0.05	−0.36 ± 0.04	0.06	0.11	0.08 ± 0.07
HD 114762	5884 ± 34	4.22 ± 0.22	1.31 ± 0.17	−0.70 ± 0.04	0.15	0.15	0.15 ± 0.09
HD 114783	5098 ± 36	4.45 ± 0.11	0.74 ± 0.05	0.09 ± 0.04	–	0.01	0.01 ± 0.07
HD 117176	5560 ± 34	4.07 ± 0.05	1.18 ± 0.05	−0.06 ± 0.05	0.11	−0.04	0.04 ± 0.10
HD 120136	6339 ± 73	4.19 ± 0.10	1.70 ± 0.16	0.23 ± 0.07	−0.18	−0.18	−0.18 ± 0.09
HD 121504	6075 ± 40	4.64 ± 0.12	1.31 ± 0.07	0.16 ± 0.05	−0.16	−0.16	−0.16 ± 0.08
HD 130322	5392 ± 36	4.48 ± 0.06	0.85 ± 0.05	0.03 ± 0.04	−0.05	−0.08	−0.06 ± 0.07
HD 134987	5776 ± 29	4.36 ± 0.07	1.09 ± 0.04	0.30 ± 0.04	−0.20	−0.15	−0.18 ± 0.07
HD 136118	6222 ± 39	4.27 ± 0.15	1.79 ± 0.12	−0.04 ± 0.05	−0.21	−0.21	−0.21 ± 0.08
HD 141937	5909 ± 39	4.51 ± 0.08	1.13 ± 0.06	0.10 ± 0.05	−0.15	−0.20	−0.18 ± 0.07
HD 142415	6045 ± 44	4.53 ± 0.08	1.12 ± 0.07	0.21 ± 0.05	−0.06	−0.11	−0.09 ± 0.08
HD 143761	5853 ± 25	4.41 ± 0.15	1.35 ± 0.07	−0.21 ± 0.04	−0.04	−0.04	−0.04 ± 0.07
HD 145675	5311 ± 87	4.42 ± 0.18	0.92 ± 0.10	0.43 ± 0.08	−0.13	−0.13	−0.13 ± 0.12
HD 147513	5883 ± 25	4.51 ± 0.05	1.18 ± 0.04	0.06 ± 0.04	–	−0.21	−0.21 ± 0.06
HD 160691	5798 ± 33	4.31 ± 0.08	1.19 ± 0.04	0.32 ± 0.04	−0.17	−0.17	−0.17 ± 0.07
HD 168443	5617 ± 35	4.22 ± 0.05	1.21 ± 0.05	0.06 ± 0.05	−0.01	−0.06	−0.04 ± 0.07
HD 168746	5601 ± 33	4.41 ± 0.12	0.99 ± 0.05	−0.08 ± 0.05	0.13	–	0.13 ± 0.07
HD 169830	6299 ± 41	4.10 ± 0.02	1.42 ± 0.09	0.21 ± 0.05	−0.31	−0.31	−0.31 ± 0.06
HD 178911	5600 ± 42	4.44 ± 0.08	0.95 ± 0.05	0.27 ± 0.05	−0.12	−0.07	−0.10 ± 0.08
HD 179949	6260 ± 43	4.43 ± 0.05	1.41 ± 0.09	0.22 ± 0.05	−0.12	−0.17	−0.15 ± 0.07
HD 186427	5772 ± 25	4.40 ± 0.07	1.07 ± 0.04	0.08 ± 0.04	−0.13	−0.13	−0.13 ± 0.06
HD 187123	5845 ± 22	4.42 ± 0.07	1.10 ± 0.03	0.13 ± 0.03	−0.28	−0.18	−0.23 ± 0.08
HD 190228	5325 ± 00	3.90 ± 0.00	1.11 ± 0.00	−0.26 ± 0.00	0.06	−0.04	0.01 ± 0.07
HD 190360	5584 ± 36	4.37 ± 0.06	1.07 ± 0.05	0.24 ± 0.05	−0.14	−0.14	−0.14 ± 0.06
HD 192263	4947 ± 58	4.51 ± 0.20	0.86 ± 0.09	−0.02 ± 0.06	−0.08	−0.08	−0.08 ± 0.10
HD 195019	5859 ± 31	4.32 ± 0.07	1.27 ± 0.05	0.09 ± 0.04	−0.24	−0.24	−0.24 ± 0.06
HD 202206	5752 ± 53	4.50 ± 0.09	1.01 ± 0.06	0.35 ± 0.06	−0.20	−0.25	−0.23 ± 0.08
HD 209458	6117 ± 26	4.48 ± 0.08	1.40 ± 0.06	0.02 ± 0.03	−0.22	−0.22	−0.22 ± 0.06

Table 6: Continued.

Star	$T_{\rm eff}$ (K)	$\log g$ (cm s^{-2})	ξ_t (km s^{-1})	[Fe/H]	[S/Fe]$_1$	[S/Fe]$_2$	[S/Fe]
HD 210277	5532 ± 00	4.29 ± 0.00	1.03 ± 0.00	0.19 ± 0.00	−0.04	−0.09	−0.07 ± 0.06
HD 213240	5984 ± 33	4.25 ± 0.10	1.25 ± 0.05	0.17 ± 0.05	−0.27	–	−0.27 ± 0.07
HD 216435	5938 ± 42	4.12 ± 0.05	1.28 ± 0.06	0.24 ± 0.05	–	−0.14	−0.14 ± 0.07
HD 216437	5887 ± 32	4.30 ± 0.07	1.31 ± 0.04	0.25 ± 0.04	–	−0.15	−0.15 ± 0.06
HD 216770	5423 ± 41	4.40 ± 0.13	1.01 ± 0.05	0.26 ± 0.04	−0.01	−0.01	−0.01 ± 0.08
HD 217014	5804 ± 36	4.42 ± 0.07	1.20 ± 0.05	0.20 ± 0.05	−0.15	−0.10	−0.13 ± 0.07
HD 217107	5645 ± 00	4.31 ± 0.00	1.06 ± 0.00	0.37 ± 0.00	−0.27	−0.22	−0.25 ± 0.06
HD 222404	4916 ± 70	3.36 ± 0.21	1.27 ± 0.06	0.16 ± 0.08	–	−0.11	−0.11 ± 0.11
HD 222582	5843 ± 38	4.45 ± 0.07	1.03 ± 0.06	0.05 ± 0.05	−0.25	–	−0.25 ± 0.07
HD 141937	5909 ± 39	4.51 ± 0.08	1.13 ± 0.06	0.10 ± 0.05	−0.15	−0.20	−0.18 ± 0.07
HD 142415	6045 ± 44	4.53 ± 0.08	1.12 ± 0.07	0.21 ± 0.05	−0.06	−0.11	−0.09 ± 0.08
HD 143761	5853 ± 25	4.41 ± 0.15	1.35 ± 0.07	−0.21 ± 0.04	−0.04	−0.04	−0.04 ± 0.07
HD 145675	5311 ± 87	4.42 ± 0.18	0.92 ± 0.10	0.43 ± 0.08	−0.13	−0.13	−0.13 ± 0.12
HD 147513	5883 ± 25	4.51 ± 0.05	1.18 ± 0.04	0.06 ± 0.04	–	−0.21	−0.21 ± 0.06
HD 160691	5798 ± 33	4.31 ± 0.08	1.19 ± 0.04	0.32 ± 0.04	−0.17	−0.17	−0.17 ± 0.07
HD 168443	5617 ± 35	4.22 ± 0.05	1.21 ± 0.05	0.06 ± 0.05	−0.01	−0.06	−0.04 ± 0.07
HD 168746	5601 ± 33	4.41 ± 0.12	0.99 ± 0.05	−0.08 ± 0.05	0.13	–	0.13 ± 0.07
HD 169830	6299 ± 41	4.10 ± 0.02	1.42 ± 0.09	0.21 ± 0.05	−0.31	−0.31	−0.31 ± 0.06
HD 178911	5600 ± 42	4.44 ± 0.08	0.95 ± 0.05	0.27 ± 0.05	−0.12	−0.07	−0.10 ± 0.08
HD 179949	6260 ± 43	4.43 ± 0.05	1.41 ± 0.09	0.22 ± 0.05	−0.12	−0.17	−0.15 ± 0.07
HD 186427	5772 ± 25	4.40 ± 0.07	1.07 ± 0.04	0.08 ± 0.04	−0.13	−0.13	−0.13 ± 0.06
HD 187123	5845 ± 22	4.42 ± 0.07	1.10 ± 0.03	0.13 ± 0.03	−0.28	−0.18	−0.23 ± 0.08
HD 190228	5325 ± 00	3.90 ± 0.00	1.11 ± 0.00	−0.26 ± 0.00	0.06	−0.04	0.01 ± 0.07
HD 190360	5584 ± 36	4.37 ± 0.06	1.07 ± 0.05	0.24 ± 0.05	−0.14	−0.14	−0.14 ± 0.06
HD 192263	4947 ± 58	4.51 ± 0.20	0.86 ± 0.09	−0.02 ± 0.06	−0.08	−0.08	−0.08 ± 0.10
HD 195019	5859 ± 31	4.32 ± 0.07	1.27 ± 0.05	0.09 ± 0.04	−0.24	−0.24	−0.24 ± 0.06
HD 202206	5752 ± 53	4.50 ± 0.09	1.01 ± 0.06	0.35 ± 0.06	−0.20	−0.25	−0.23 ± 0.08
HD 209458	6117 ± 26	4.48 ± 0.08	1.40 ± 0.06	0.02 ± 0.03	−0.22	−0.22	−0.22 ± 0.06
HD 210277	5532 ± 00	4.29 ± 0.00	1.03 ± 0.00	0.19 ± 0.00	−0.04	−0.09	−0.07 ± 0.06
HD 213240	5984 ± 33	4.25 ± 0.10	1.25 ± 0.05	0.17 ± 0.05	−0.27	–	−0.27 ± 0.07
HD 216435	5938 ± 42	4.12 ± 0.05	1.28 ± 0.06	0.24 ± 0.05	–	−0.14	−0.14 ± 0.07
HD 216437	5887 ± 32	4.30 ± 0.07	1.31 ± 0.04	0.25 ± 0.04	–	−0.15	−0.15 ± 0.06
HD 216770	5423 ± 41	4.40 ± 0.13	1.01 ± 0.05	0.26 ± 0.04	−0.01	−0.01	−0.01 ± 0.08
HD 217014	5804 ± 36	4.42 ± 0.07	1.20 ± 0.05	0.20 ± 0.05	−0.15	−0.10	−0.13 ± 0.07
HD 217107	5645 ± 00	4.31 ± 0.00	1.06 ± 0.00	0.37 ± 0.00	−0.27	−0.22	−0.25 ± 0.06
HD 222404	4916 ± 70	3.36 ± 0.21	1.27 ± 0.06	0.16 ± 0.08	–	−0.11	−0.11 ± 0.11
HD 222582	5843 ± 38	4.45 ± 0.07	1.03 ± 0.06	0.05 ± 0.05	−0.25	–	−0.25 ± 0.07

Table 7: Sulphur abundances from SI lines 6743 Å and 6757 Å for a set of comparison stars.

Star	$T_{\rm eff}$ (K)	$\log g$ (cm s^{-2})	ξ_t (km s^{-1})	[Fe/H]	[S/Fe]$_1$	[S/Fe]$_2$	[S/Fe]
HD 1581	5956 ± 44	4.39 ± 0.13	1.07 ± 0.09	−0.14 ± 0.05	−0.16	−0.11	−0.28 ± 0.08
HD 4391	5878 ± 53	4.74 ± 0.15	1.13 ± 0.10	−0.03 ± 0.06	–	−0.02	−0.02 ± 0.09
HD 5133	4911 ± 54	4.49 ± 0.18	0.71 ± 0.11	−0.17 ± 0.06	−0.23	−0.23	−0.23 ± 0.09
HD 7570	6140 ± 41	4.39 ± 0.16	1.50 ± 0.08	0.18 ± 0.05	−0.18	−0.18	−0.18 ± 0.08
HD 10360	4970 ± 40	4.49 ± 0.10	0.76 ± 0.07	−0.26 ± 0.04	–	0.06	0.06 ± 0.07
HD 10700	5344 ± 29	4.57 ± 0.09	0.91 ± 0.06	−0.52 ± 0.04	0.02	0.12	0.07 ± 0.08
HD 14412	5368 ± 24	4.55 ± 0.05	0.88 ± 0.05	−0.47 ± 0.03	0.07	0.07	0.07 ± 0.06
HD 17925	5180 ± 56	4.44 ± 0.13	1.33 ± 0.08	0.06 ± 0.07	−0.16	−0.11	−0.14 ± 0.09
HD 20010	6275 ± 57	4.40 ± 0.37	2.41 ± 0.41	−0.19 ± 0.06	0.04	−0.01	0.02 ± 0.15

Table 7: Continued.

Star	$T_{\rm eff}$ (K)	$\log g$ (cm s^{-2})	ξ_t (km s^{-1})	[Fe/H]	[S/Fe]$_1$	[S/Fe]$_2$	[S/Fe]
HD 20766	5733 ± 31	4.55 ± 0.10	1.09 ± 0.06	−0.21 ± 0.04	–	−0.09	−0.09 ± 0.07
HD 20794	5444 ± 31	4.47 ± 0.07	0.98 ± 0.06	−0.38 ± 0.04	–	0.03	0.03 ± 0.06
HD 20807	5843 ± 26	4.47 ± 0.10	1.17 ± 0.06	−0.23 ± 0.04	−0.07	−0.07	−0.07 ± 0.07
HD 23249	5074 ± 60	3.77 ± 0.16	1.08 ± 0.06	0.13 ± 0.08	–	−0.18	−0.18 ± 0.09
HD 23484	5176 ± 45	4.41 ± 0.17	1.03 ± 0.06	0.06 ± 0.05	–	−0.16	−0.16 ± 0.09
HD 30495	5868 ± 30	4.55 ± 0.10	1.24 ± 0.05	0.02 ± 0.04	−0.12	−0.12	−0.12 ± 0.07
HD 36435	5479 ± 37	4.61 ± 0.07	1.12 ± 0.05	0.00 ± 0.05	–	−0.05	−0.05 ± 0.07
HD 38858	5752 ± 32	4.53 ± 0.07	1.26 ± 0.07	−0.23 ± 0.05	−0.02	−0.02	−0.02 ± 0.06
HD 43162	5633 ± 35	4.48 ± 0.07	1.24 ± 0.05	−0.01 ± 0.04	−0.19	−0.14	−0.17 ± 0.07
HD 43834	5594 ± 36	4.41 ± 0.09	1.05 ± 0.04	0.10 ± 0.10	−0.05	−0.05	−0.05 ± 0.07
HD 53705	5825 ± 20	4.37 ± 0.10	1.20 ± 0.04	−0.19 ± 0.03	−0.01	−0.01	−0.01 ± 0.06
HD 53706	5260 ± 31	4.35 ± 0.11	0.74 ± 0.05	−0.26 ± 0.04	0.16	0.16	0.16 ± 0.07
HD 65907	5979 ± 31	4.59 ± 0.12	1.36 ± 0.10	−0.29 ± 0.04	–	0.04	0.04 ± 0.07
HD 69830	5410 ± 26	4.38 ± 0.07	0.89 ± 0.03	−0.03 ± 0.04	−0.12	−0.12	−0.12 ± 0.06
HD 74576	5000 ± 55	4.55 ± 0.13	1.07 ± 0.08	−0.03 ± 0.06	–	−0.07	−0.07 ± 0.09
HD 76151	5803 ± 29	4.50 ± 0.08	1.02 ± 0.04	0.14 ± 0.04	−0.04	−0.04	−0.04 ± 0.06
HD 84117	6167 ± 37	4.35 ± 0.10	1.42 ± 0.09	−0.03 ± 0.05	−0.07	−0.07	−0.07 ± 0.07
HD 189567	5765 ± 24	4.52 ± 0.05	1.22 ± 0.05	−0.23 ± 0.04	–	−0.07	−0.07 ± 0.06
HD 192310	5069 ± 49	4.38 ± 0.19	0.79 ± 0.07	−0.01 ± 0.05	–	−0.29	−0.29 ± 0.09
HD 196761	5435 ± 39	4.48 ± 0.08	0.91 ± 0.07	−0.29 ± 0.05	–	−0.01	−0.01 ± 0.07
HD 207129	5910 ± 24	4.42 ± 0.05	1.14 ± 0.04	0.00 ± 0.04	−0.05	−0.05	−0.05 ± 0.06
HD 211415	5890 ± 30	4.51 ± 0.07	1.12 ± 0.07	−0.17 ± 0.04	−0.03	−0.03	−0.03 ± 0.06

Table 8: Zn abundances from ZnI lines at 4810 Å and 4722 Å for a set of stars with planets and brown dwarf companions.

Star	$T_{\rm eff}$ (K)	$\log g$ (cm s^{-2})	ξ_t (km s^{-1})	[Fe/H]	[Zn/Fe]$_1$	[Zn/Fe]$_2$	[Zn/Fe]
HD 142	6302 ± 56	4.34 ± 0.13	1.86 ± 0.17	0.14 ± 0.07	−0.25	−0.16	−0.21 ± 0.10
HD 2039	5976 ± 51	4.45 ± 0.10	1.26 ± 0.07	0.32 ± 0.06	−0.05	−0.03	−0.04 ± 0.07
HD 4203	5636 ± 40	4.23 ± 0.14	1.12 ± 0.05	0.40 ± 0.05	0.00	0.02	0.01 ± 0.07
HD 4208	5626 ± 32	4.49 ± 0.10	0.95 ± 0.06	−0.24 ± 0.04	0.12	0.22	0.17 ± 0.08
HD 6434	5835 ± 59	4.60 ± 0.12	1.53 ± 0.27	−0.52 ± 0.08	0.05	0.07	0.06 ± 0.10
HD 8574	6151 ± 57	4.51 ± 0.10	1.45 ± 0.15	0.06 ± 0.07	−0.17	−0.08	−0.13 ± 0.10
HD 9826	6212 ± 64	4.26 ± 0.13	1.69 ± 0.16	0.13 ± 0.08	−0.15	−0.08	−0.12 ± 0.10
HD 10647	6143 ± 31	4.48 ± 0.08	1.40 ± 0.08	−0.03 ± 0.04	−0.10	−0.16	−0.13 ± 0.07
HD 10697	5641 ± 28	4.05 ± 0.05	1.13 ± 0.03	0.14 ± 0.04	0.08	0.12	0.10 ± 0.06
HD 12661	5702 ± 36	4.33 ± 0.08	1.05 ± 0.04	0.36 ± 0.05	0.08	0.17	0.13 ± 0.08
HD 13445	5163 ± 00	4.52 ± 0.00	0.72 ± 0.00	−0.24 ± 0.00	0.20	0.21	0.21 ± 0.06
HD 16141	5801 ± 30	4.22 ± 0.12	1.34 ± 0.04	0.15 ± 0.04	−0.05	−0.08	−0.07 ± 0.07
HD 17051	6252 ± 53	4.61 ± 0.16	1.18 ± 0.10	0.26 ± 0.06	−0.04	−0.08	−0.06 ± 0.08
HD 19994	6190 ± 00	4.19 ± 0.00	1.54 ± 0.00	0.24 ± 0.00	−0.15	−0.08	−0.12 ± 0.09
HD 20367	6138 ± 79	4.53 ± 0.22	1.22 ± 0.16	0.17 ± 0.10	−0.10	−0.08	−0.09 ± 0.11
HD 22049	5073 ± 42	4.43 ± 0.08	1.05 ± 0.06	−0.13 ± 0.05	−0.15	−0.08	−0.12 ± 0.08
HD 23079	5959 ± 46	4.35 ± 0.12	1.20 ± 0.10	−0.11 ± 0.06	−0.10	−0.05	−0.08 ± 0.08
HD 23596	6108 ± 36	4.25 ± 0.10	1.30 ± 0.05	0.31 ± 0.05	−0.05	−0.08	−0.07 ± 0.07
HD 27442	4825 ± 107	3.55 ± 0.32	1.18 ± 0.12	0.39 ± 0.13	−0.18	−0.08	−0.13 ± 0.15
HD 28185	5656 ± 44	4.45 ± 0.08	1.01 ± 0.06	0.22 ± 0.05	0.10	0.07	0.09 ± 0.07
HD 30177	5587 ± 00	4.29 ± 0.00	1.08 ± 0.00	0.38 ± 0.00	0.05	0.07	0.06 ± 0.07
HD 33636	6046 ± 49	4.71 ± 0.09	1.79 ± 0.19	−0.08 ± 0.06	−0.32	−0.25	−0.29 ± 0.09
HD 37124	5546 ± 30	4.50 ± 0.03	0.80 ± 0.07	−0.38 ± 0.04	0.15	0.32	0.24 ± 0.11
HD 38529	5674 ± 40	3.94 ± 0.12	1.38 ± 0.05	0.40 ± 0.06	−0.17	−0.10	−0.14 ± 0.08

Table 8: Continued.

Star	$T_{\rm eff}$ (K)	log g (cm s^{-2})	ξ_t (km s^{-1})	[Fe/H]	[Zn/Fe]$_1$	[Zn/Fe]$_2$	[Zn/Fe]
HD 39091	5991 ± 27	4.42 ± 0.10	1.24 ± 0.04	0.10 ± 0.04	0.00	−0.03	−0.02 ± 0.07
HD 40979	5115 ± 68	4.32 ± 0.19	0.93 ± 0.09	0.04 ± 0.07	−0.15	0.00	−0.08 ± 0.12
HD 46375	5268 ± 55	4.41 ± 0.16	0.97 ± 0.06	0.20 ± 0.06	0.10	0.17	0.14 ± 0.09
HD 49674	5644 ± 54	4.37 ± 0.07	0.89 ± 0.07	0.33 ± 0.06	−0.05	−0.01	−0.03 ± 0.07
HD 50554	6026 ± 30	4.41 ± 0.13	1.11 ± 0.06	0.01 ± 0.04	0.10	0.12	0.11 ± 0.07
HD 52265	6105 ± 00	4.28 ± 0.00	1.36 ± 0.00	0.23 ± 0.00	−0.07	−0.10	−0.09 ± 0.07
HD 73256	5608 ± 34	4.35 ± 0.08	1.24 ± 0.04	0.26 ± 0.04	−0.10	−0.04	−0.07 ± 0.07
HD 74156	6112 ± 39	4.34 ± 0.10	1.38 ± 0.07	0.16 ± 0.05	−0.05	−0.03	−0.04 ± 0.07
HD 75732	5279 ± 62	4.37 ± 0.18	0.98 ± 0.07	0.33 ± 0.07	0.15	0.17	0.16 ± 0.09
HD 80606	5574 ± 72	4.46 ± 0.20	1.14 ± 0.09	0.32 ± 0.09	0.05	0.02	0.04 ± 0.10
HD 92788	5821 ± 41	4.45 ± 0.06	1.16 ± 0.05	0.32 ± 0.05	0.10	0.12	0.11 ± 0.07
HD 95128	5954 ± 25	4.44 ± 0.10	1.30 ± 0.04	0.06 ± 0.03	−0.03	0.02	0.00 ± 0.07
HD 106252	5899 ± 35	4.34 ± 0.07	1.08 ± 0.06	−0.01 ± 0.05	−0.10	−0.16	−0.13 ± 0.07
HD 108147	6248 ± 42	4.49 ± 0.16	1.35 ± 0.08	0.20 ± 0.05	−0.15	−0.13	−0.14 ± 0.08
HD 114386	4804 ± 61	4.36 ± 0.28	0.57 ± 0.12	−0.08 ± 0.06	0.30	0.12	0.21 ± 0.13
HD 114783	5098 ± 36	4.45 ± 0.11	0.74 ± 0.05	0.09 ± 0.04	0.15	0.20	0.18 ± 0.07
HD 121504	6075 ± 40	4.64 ± 0.12	1.31 ± 0.07	0.16 ± 0.05	0.04	0.06	0.05 ± 0.07
HD 130322	5392 ± 36	4.48 ± 0.06	0.85 ± 0.05	0.03 ± 0.04	−0.05	0.17	0.06 ± 0.13
HD 134987	5776 ± 29	4.36 ± 0.07	1.09 ± 0.04	0.30 ± 0.04	0.15	0.22	0.19 ± 0.07
HD 136118	6222 ± 39	4.27 ± 0.15	1.79 ± 0.12	−0.04 ± 0.05	−0.25	−0.15	−0.20 ± 0.09
HD 137759	4775 ± 110	3.09 ± 0.40	1.78 ± 0.11	0.13 ± 0.14	−0.36	−0.26	−0.31 ± 0.16
HD 141937	5909 ± 39	4.51 ± 0.08	1.13 ± 0.06	0.10 ± 0.05	−0.05	0.02	−0.02 ± 0.08
HD 143761	5853 ± 25	4.41 ± 0.15	1.35 ± 0.07	−0.21 ± 0.04	0.07	0.12	0.10 ± 0.08
HD 145675	5311 ± 87	4.42 ± 0.18	0.92 ± 0.10	0.43 ± 0.08	0.10	0.22	0.16 ± 0.11
HD 147513	5883 ± 25	4.51 ± 0.05	1.18 ± 0.04	0.06 ± 0.04	−0.10	−0.08	−0.09 ± 0.06
HD 160691	5798 ± 33	4.31 ± 0.08	1.19 ± 0.04	0.32 ± 0.04	0.00	0.00	0.00 ± 0.06
HD 168443	5617 ± 35	4.22 ± 0.05	1.21 ± 0.05	0.06 ± 0.05	0.15	0.17	0.16 ± 0.07
HD 168746	5601 ± 33	4.41 ± 0.12	0.99 ± 0.05	−0.08 ± 0.05	0.10	0.17	0.14 ± 0.08
HD 177830	4804 ± 77	3.57 ± 0.17	1.14 ± 0.09	0.33 ± 0.09	−0.08	0.10	0.01 ± 0.13
HD 178911	5588 ± 115	4.46 ± 0.20	0.82 ± 0.14	0.24 ± 0.10	0.01	0.03	0.02 ± 0.11
HD 179949	6260 ± 43	4.43 ± 0.05	1.41 ± 0.09	0.22 ± 0.05	−0.39	−0.38	−0.39 ± 0.07
HD 186427	5772 ± 25	4.40 ± 0.07	1.07 ± 0.04	0.08 ± 0.04	0.10	0.12	0.11 ± 0.06
HD 187123	5845 ± 22	4.42 ± 0.07	1.10 ± 0.03	0.13 ± 0.03	0.10	0.05	0.08 ± 0.06
HD 190360	5584 ± 36	4.37 ± 0.06	1.07 ± 0.05	0.24 ± 0.05	0.05	0.07	0.06 ± 0.07
HD 192263	4947 ± 58	4.51 ± 0.20	0.86 ± 0.09	−0.02 ± 0.06	0.06	0.07	0.07 ± 0.09
HD 195019	5859 ± 31	4.32 ± 0.07	1.27 ± 0.05	0.09 ± 0.04	−0.05	−0.08	−0.07 ± 0.06
HD 196050	5918 ± 44	4.35 ± 0.13	1.39 ± 0.06	0.22 ± 0.05	0.00	0.02	0.01 ± 0.07
HD 210277	5532 ± 00	4.29 ± 0.00	1.03 ± 0.00	0.19 ± 0.00	0.05	0.12	0.09 ± 0.07
HD 213240	5984 ± 33	4.25 ± 0.10	1.25 ± 0.05	0.17 ± 0.05	−0.05	−0.03	−0.04 ± 0.07
HD 216435	5938 ± 42	4.12 ± 0.05	1.28 ± 0.06	0.24 ± 0.05	−0.05	−0.03	−0.04 ± 0.07
HD 216437	5887 ± 32	4.30 ± 0.07	1.31 ± 0.04	0.25 ± 0.04	0.00	0.02	0.01 ± 0.06
HD 217014	5804 ± 36	4.42 ± 0.07	1.20 ± 0.05	0.20 ± 0.05	−0.02	−0.01	−0.02 ± 0.07
HD 217107	5645 ± 00	4.31 ± 0.00	1.06 ± 0.00	0.37 ± 0.00	0.00	0.07	0.04 ± 0.07
HD 222582	5843 ± 38	4.45 ± 0.07	1.03 ± 0.06	0.05 ± 0.05	−0.05	−0.03	−0.04 ± 0.07

Table 9: Zn abundances from ZnI lines at 4810 Å and 4722 Å for a set of comparison stars.

Star	$T_{\rm eff}$ (K)	log g (cm s^{-2})	ξ_t (km s^{-1})	[Fe/H]	[Zn/Fe]$_1$	[Zn/Fe]$_2$	[Zn/Fe]
HD 1581	5956 ± 44	4.39 ± 0.13	1.07 ± 0.09	−0.14 ± 0.05	0.09	0.06	0.08 ± 0.08
HD 4391	5878 ± 53	4.74 ± 0.15	1.13 ± 0.10	−0.03 ± 0.06	−0.05	−0.08	−0.07 ± 0.08

Table 9: Continued.

Star	$T_{\rm eff}$ (K)	$\log g$ (cm s^{-2})	ξ_t (km s^{-1})	[Fe/H]	[Zn/Fe]$_1$	[Zn/Fe]$_2$	[Zn/Fe]
HD 5133	4911 ± 54	4.49 ± 0.18	0.71 ± 0.11	−0.17 ± 0.06	−0.05	−0.03	−0.04 ± 0.08
HD 7570	6140 ± 41	4.39 ± 0.16	1.50 ± 0.08	0.18 ± 0.05	−0.05	−0.13	−0.09 ± 0.08
HD 10360	4970 ± 40	4.49 ± 0.10	0.76 ± 0.07	−0.26 ± 0.04	0.00	0.05	0.03 ± 0.07
HD 10700	5344 ± 29	4.57 ± 0.09	0.91 ± 0.06	−0.52 ± 0.04	0.15	0.19	0.17 ± 0.07
HD 14412	5368 ± 24	4.55 ± 0.05	0.88 ± 0.05	−0.47 ± 0.03	0.03	0.09	0.06 ± 0.06
HD 17925	5180 ± 56	4.44 ± 0.13	1.33 ± 0.08	0.06 ± 0.07	−0.10	−0.11	−0.11 ± 0.08
HD 20010	6275 ± 57	4.40 ± 0.37	2.41 ± 0.41	−0.19 ± 0.06	−0.35	−0.28	−0.32 ± 0.14
HD 20766	5733 ± 31	4.55 ± 0.10	1.09 ± 0.06	−0.21 ± 0.04	0.00	0.02	0.01 ± 0.06
HD 20794	5444 ± 31	4.47 ± 0.07	0.98 ± 0.06	−0.38 ± 0.04	0.20	0.20	0.20 ± 0.06
HD 20807	5843 ± 26	4.47 ± 0.10	1.17 ± 0.06	−0.23 ± 0.04	−0.05	−0.05	−0.05 ± 0.06
HD 23249	5074 ± 60	3.77 ± 0.16	1.08 ± 0.06	0.13 ± 0.08	−0.05	0.07	0.01 ± 0.11
HD 23356	4975 ± 55	4.48 ± 0.16	0.77 ± 0.09	−0.11 ± 0.06	−0.12	0.03	−0.05 ± 0.11
HD 23484	5176 ± 45	4.41 ± 0.17	1.03 ± 0.06	0.06 ± 0.05	−0.08	−0.03	−0.06 ± 0.08
HD 26965	5126 ± 34	4.51 ± 0.08	0.60 ± 0.07	−0.31 ± 0.04	0.30	0.22	0.26 ± 0.07
HD 30495	5868 ± 30	4.55 ± 0.10	1.24 ± 0.05	0.02 ± 0.04	−0.13	−0.08	−0.11 ± 0.07
HD 36435	5479 ± 37	4.61 ± 0.07	1.12 ± 0.05	−0.00 ± 0.05	−0.08	−0.15	−0.12 ± 0.08
HD 38858	5752 ± 32	4.53 ± 0.07	1.26 ± 0.07	−0.23 ± 0.05	−0.05	−0.08	−0.07 ± 0.07
HD 40307	4805 ± 52	4.37 ± 0.37	0.49 ± 0.12	−0.30 ± 0.05	0.10	0.12	0.11 ± 0.11
HD 43162	5633 ± 35	4.48 ± 0.07	1.24 ± 0.05	−0.01 ± 0.04	−0.10	−0.08	−0.09 ± 0.06
HD 43834	5594 ± 36	4.41 ± 0.09	1.05 ± 0.04	0.10 ± 0.05	0.05	0.07	0.06 ± 0.07
HD 50281	4658 ± 56	4.32 ± 0.24	0.64 ± 0.15	−0.04 ± 0.07	0.00	0.07	0.04 ± 0.10
HD 53705	5825 ± 20	4.37 ± 0.10	1.20 ± 0.04	−0.19 ± 0.03	0.00	0.02	0.01 ± 0.06
HD 53706	5260 ± 31	4.35 ± 0.11	0.74 ± 0.05	−0.26 ± 0.04	0.15	0.22	0.19 ± 0.08
HD 65907	5979 ± 31	4.59 ± 0.12	1.36 ± 0.10	−0.29 ± 0.04	0.05	0.17	0.11 ± 0.09
HD 69830	5410 ± 26	4.38 ± 0.07	0.89 ± 0.03	−0.03 ± 0.04	0.03	0.07	0.05 ± 0.06
HD 72673	5242 ± 28	4.50 ± 0.09	0.69 ± 0.05	−0.37 ± 0.04	0.10	0.09	0.10 ± 0.06
HD 74576	5000 ± 55	4.55 ± 0.13	1.07 ± 0.08	−0.03 ± 0.06	−0.10	−0.08	−0.09 ± 0.08
HD 76151	5803 ± 29	4.50 ± 0.08	1.02 ± 0.04	0.14 ± 0.04	0.07	0.07	0.07 ± 0.06
HD 84117	6167 ± 37	4.35 ± 0.10	1.42 ± 0.09	−0.03 ± 0.05	−0.10	−0.08	−0.09 ± 0.07
HD 189567	5765 ± 24	4.52 ± 0.05	1.22 ± 0.05	−0.23 ± 0.04	0.00	0.02	0.01 ± 0.06
HD 191408	5005 ± 45	4.38 ± 0.25	0.67 ± 0.09	−0.55 ± 0.06	0.25	0.17	0.21 ± 0.10
HD 192310	5069 ± 49	4.38 ± 0.19	0.79 ± 0.07	−0.01 ± 0.05	0.10	0.17	0.14 ± 0.09
HD 196761	5435 ± 39	4.48 ± 0.08	0.91 ± 0.07	−0.29 ± 0.05	0.10	0.07	0.09 ± 0.07
HD 207129	5910 ± 24	4.42 ± 0.05	1.14 ± 0.04	0.00 ± 0.04	−0.08	−0.13	−0.11 ± 0.07
HD 209100	4629 ± 77	4.36 ± 0.19	0.42 ± 0.25	−0.06 ± 0.08	0.10	0.09	0.10 ± 0.11
HD 211415	5890 ± 30	4.51 ± 0.07	1.12 ± 0.07	−0.17 ± 0.04	−0.05	−0.08	−0.07 ± 0.07
HD 216803	4555 ± 87	4.53 ± 0.26	0.66 ± 0.28	−0.01 ± 0.09	0.04	0.03	0.04 ± 0.12
HD 222237	4747 ± 58	4.48 ± 0.22	0.40 ± 0.20	−0.31 ± 0.06	0.26	0.18	0.22 ± 0.10
HD 222335	5260 ± 41	4.45 ± 0.11	0.92 ± 0.06	−0.16 ± 0.05	0.04	0.03	0.04 ± 0.07

Table 10: Cu abundances from CuI lines at 5218 Å and 5782 Å for a set of stars with planets and brown dwarf companions.

Star	$T_{\rm eff}$ (K)	$\log g$ (cm s^{-2})	ξ_t (km s^{-1})	[Fe/H]	[Cu/Fe]$_1$	[Cu/Fe]$_2$	[Cu/Fe]
HD 142	6302 ± 56	4.34 ± 0.13	1.86 ± 0.17	0.14 ± 0.07	−0.06	0.04	−0.01 ± 0.10
HD 2039	5976 ± 51	4.45 ± 0.10	1.26 ± 0.07	0.32 ± 0.06	0.08	0.12	0.10 ± 0.08
HD 4203	5636 ± 40	4.23 ± 0.14	1.12 ± 0.05	0.40 ± 0.05	0.20	0.10	0.15 ± 0.08
HD 4208	5626 ± 32	4.49 ± 0.10	0.95 ± 0.06	−0.24 ± 0.04	0.06	0.07	0.07 ± 0.06
HD 6434	5835 ± 59	4.60 ± 0.12	1.53 ± 0.27	−0.52 ± 0.08	0.00	0.08	0.04 ± 0.11
HD 8574	6151 ± 57	4.51 ± 0.10	1.45 ± 0.15	0.06 ± 0.07	0.00	0.04	0.02 ± 0.09
HD 9826	6212 ± 64	4.26 ± 0.13	1.69 ± 0.16	0.13 ± 0.08	−0.05	0.02	−0.02 ± 0.10

Table 10: Continued.

Star	$T_{\rm eff}$ (K)	$\log g$ (cm s^{-2})	ξ_t (km s^{-1})	[Fe/H]	[Cu/Fe]$_1$	[Cu/Fe]$_2$	[Cu/Fe]
HD 10647	6143 ± 31	4.48 ± 0.08	1.40 ± 0.08	−0.03 ± 0.04	−0.13	−0.03	−0.08 ± 0.08
HD 10697	5641 ± 28	4.05 ± 0.05	1.13 ± 0.03	0.14 ± 0.04	0.05	0.00	0.03 ± 0.07
HD 12661	5702 ± 36	4.33 ± 0.08	1.05 ± 0.04	0.36 ± 0.05	0.20	0.12	0.16 ± 0.08
HD 13445	5163 ± 00	4.52 ± 0.00	0.72 ± 0.00	−0.24 ± 0.00	0.40	0.06	0.23 ± 0.18
HD 16141	5801 ± 30	4.22 ± 0.12	1.34 ± 0.04	0.15 ± 0.04	−0.05	0.03	−0.01 ± 0.07
HD 17051	6252 ± 53	4.61 ± 0.16	1.18 ± 0.10	0.26 ± 0.06	−0.05	0.02	−0.02 ± 0.09
HD 19994	6190 ± 00	4.19 ± 0.00	1.54 ± 0.00	0.24 ± 0.00	0.05	0.12	0.09 ± 0.06
HD 20367	6138 ± 79	4.53 ± 0.22	1.22 ± 0.16	0.17 ± 0.10	−0.05	−0.08	−0.07 ± 0.11
HD 22049	5073 ± 42	4.43 ± 0.08	1.05 ± 0.06	−0.13 ± 0.05	0.00	0.02	0.01 ± 0.07
HD 23079	5959 ± 46	4.35 ± 0.12	1.20 ± 0.10	−0.11 ± 0.06	−0.05	−0.02	−0.04 ± 0.08
HD 23596	6108 ± 36	4.25 ± 0.10	1.30 ± 0.05	0.31 ± 0.05	0.15	0.18	0.17 ± 0.07
HD 27442	4825 ± 107	3.55 ± 0.32	1.18 ± 0.12	0.39 ± 0.13	0.20	0.24	0.22 ± 0.13
HD 28185	5656 ± 44	4.45 ± 0.08	1.01 ± 0.06	0.22 ± 0.05	0.15	0.13	0.14 ± 0.07
HD 30177	5587 ± 00	4.29 ± 0.00	1.08 ± 0.00	0.38 ± 0.00	0.15	0.07	0.11 ± 0.06
HD 33636	6046 ± 49	4.71 ± 0.09	1.79 ± 0.19	−0.08 ± 0.06	−0.03	0.03	0.00 ± 0.09
HD 37124	5546 ± 30	4.50 ± 0.03	0.80 ± 0.07	−0.38 ± 0.04	0.08	0.09	0.09 ± 0.06
HD 38529	5674 ± 40	3.94 ± 0.12	1.38 ± 0.05	0.40 ± 0.06	0.15	0.10	0.13 ± 0.08
HD 39091	5991 ± 27	4.42 ± 0.10	1.24 ± 0.04	0.10 ± 0.04	0.05	0.09	0.07 ± 0.06
HD 40979	5115 ± 68	4.32 ± 0.19	0.93 ± 0.09	0.04 ± 0.07	0.00	−0.05	−0.03 ± 0.09
HD 46375	5268 ± 55	4.41 ± 0.16	0.97 ± 0.06	0.20 ± 0.06	0.14	0.14	0.14 ± 0.08
HD 49674	5644 ± 54	4.37 ± 0.07	0.89 ± 0.07	0.33 ± 0.06	−0.13	−0.11	−0.12 ± 0.07
HD 50554	6026 ± 30	4.41 ± 0.13	1.11 ± 0.06	0.01 ± 0.04	0.00	0.00	0.00 ± 0.06
HD 52265	6105 ± 00	4.28 ± 0.00	1.36 ± 0.00	0.23 ± 0.00	0.10	0.08	0.09 ± 0.05
HD 73256	5608 ± 34	4.35 ± 0.08	1.24 ± 0.04	0.26 ± 0.04	−0.01	0.01	0.00 ± 0.06
HD 74156	6112 ± 39	4.34 ± 0.10	1.38 ± 0.07	0.16 ± 0.05	0.05	0.08	0.07 ± 0.07
HD 75732	5279 ± 62	4.37 ± 0.18	0.98 ± 0.07	0.33 ± 0.07	0.15	0.10	0.13 ± 0.09
HD 80606	5574 ± 72	4.46 ± 0.20	1.14 ± 0.09	0.32 ± 0.09	0.20	0.22	0.21 ± 0.10
HD 89744	6234 ± 45	3.98 ± 0.05	1.62 ± 0.08	0.22 ± 0.05	−	0.00	0.00 ± 0.07
HD 92788	5821 ± 41	4.45 ± 0.06	1.16 ± 0.05	0.32 ± 0.05	0.20	0.17	0.19 ± 0.07
HD 95128	5954 ± 25	4.44 ± 0.10	1.30 ± 0.04	0.06 ± 0.03	0.05	0.12	0.09 ± 0.07
HD 106252	5899 ± 35	4.34 ± 0.07	1.08 ± 0.06	−0.01 ± 0.05	−0.05	0.01	−0.02 ± 0.07
HD 108147	6248 ± 42	4.49 ± 0.16	1.35 ± 0.08	0.20 ± 0.05	−0.05	0.00	−0.03 ± 0.08
HD 108874	5596 ± 42	4.37 ± 0.12	0.89 ± 0.05	0.23 ± 0.05	0.10	0.09	0.10 ± 0.07
HD 114386	4804 ± 61	4.36 ± 0.28	0.57 ± 0.12	−0.08 ± 0.06	0.13	0.10	0.12 ± 0.09
HD 114729	5886 ± 36	4.28 ± 0.13	1.25 ± 0.09	−0.25 ± 0.05	0.00	0.05	0.03 ± 0.08
HD 114783	5098 ± 36	4.45 ± 0.11	0.74 ± 0.05	0.09 ± 0.04	0.15	0.09	0.12 ± 0.07
HD 121504	6075 ± 40	4.64 ± 0.12	1.31 ± 0.07	0.16 ± 0.05	−0.01	0.03	0.01 ± 0.07
HD 128311	4835 ± 72	4.44 ± 0.21	0.89 ± 0.11	0.03 ± 0.07	−0.03	−0.05	−0.04 ± 0.09
HD 130322	5392 ± 36	4.48 ± 0.06	0.85 ± 0.05	0.03 ± 0.04	0.05	0.00	0.03 ± 0.07
HD 134987	5776 ± 29	4.36 ± 0.07	1.09 ± 0.04	0.30 ± 0.04	0.20	0.17	0.19 ± 0.06
HD 136118	6222 ± 39	4.27 ± 0.15	1.79 ± 0.12	−0.04 ± 0.05	0.00	0.08	0.04 ± 0.08
HD 137759	4775 ± 110	3.09 ± 0.40	1.78 ± 0.11	0.13 ± 0.14	0.07	0.09	0.08 ± 0.14
HD 141937	5909 ± 39	4.51 ± 0.08	1.13 ± 0.06	0.10 ± 0.05	0.05	0.09	0.07 ± 0.07
HD 143761	5853 ± 25	4.41 ± 0.15	1.35 ± 0.07	−0.21 ± 0.04	0.05	0.08	0.07 ± 0.07
HD 145675	5311 ± 87	4.42 ± 0.18	0.92 ± 0.10	0.43 ± 0.08	0.20	0.17	0.19 ± 0.10
HD 147513	5883 ± 25	4.51 ± 0.05	1.18 ± 0.04	0.06 ± 0.04	−0.12	−0.07	−0.10 ± 0.07
HD 150706	5961 ± 27	4.50 ± 0.10	1.11 ± 0.06	−0.01 ± 0.04	−0.15	−0.08	−0.12 ± 0.07
HD 160691	5798 ± 33	4.31 ± 0.08	1.19 ± 0.04	0.32 ± 0.04	0.12	0.10	0.11 ± 0.06
HD 168443	5617 ± 35	4.22 ± 0.05	1.21 ± 0.05	0.06 ± 0.05	0.15	0.13	0.14 ± 0.07
HD 168746	5601 ± 33	4.41 ± 0.12	0.99 ± 0.05	−0.08 ± 0.05	0.10	0.10	0.10 ± 0.07
HD 177830	4804 ± 77	3.57 ± 0.17	1.14 ± 0.09	0.33 ± 0.09	0.17	0.24	0.21 ± 0.10
HD 178911	5588 ± 115	4.46 ± 0.20	0.82 ± 0.14	0.24 ± 0.10	−0.14	−0.17	−0.16 ± 0.11
HD 179949	6260 ± 43	4.43 ± 0.05	1.41 ± 0.09	0.22 ± 0.05	−0.05	−0.03	−0.04 ± 0.07

Table 10: Continued.

Star	$T_{\rm eff}$ (K)	$\log g$ (cm s^{-2})	ξ_t (km s^{-1})	[Fe/H]	[Cu/Fe]$_1$	[Cu/Fe]$_2$	[Cu/Fe]
HD 186427	5772 ± 25	4.40 ± 0.07	1.07 ± 0.04	0.08 ± 0.04	0.12	0.12	0.12 ± 0.06
HD 187123	5845 ± 22	4.42 ± 0.07	1.10 ± 0.03	0.13 ± 0.03	0.05	0.09	0.07 ± 0.06
HD 190360	5584 ± 36	4.37 ± 0.06	1.07 ± 0.05	0.24 ± 0.05	0.15	0.09	0.12 ± 0.07
HD 192263	4947 ± 58	4.51 ± 0.20	0.86 ± 0.09	−0.02 ± 0.06	0.00	0.02	0.01 ± 0.08
HD 195019	5859 ± 31	4.32 ± 0.07	1.27 ± 0.05	0.09 ± 0.04	0.00	0.05	0.03 ± 0.07
HD 196050	5918 ± 44	4.35 ± 0.13	1.39 ± 0.06	0.22 ± 0.05	0.22	0.17	0.20 ± 0.08
HD 210277	5532 ± 00	4.29 ± 0.00	1.03 ± 0.00	0.19 ± 0.00	0.15	0.12	0.14 ± 0.06
HD 213240	5984 ± 33	4.25 ± 0.10	1.25 ± 0.05	0.17 ± 0.05	0.08	0.07	0.08 ± 0.07
HD 216435	5938 ± 42	4.12 ± 0.05	1.28 ± 0.06	0.24 ± 0.05	−0.02	0.05	0.02 ± 0.08
HD 216437	5887 ± 32	4.30 ± 0.07	1.31 ± 0.04	0.25 ± 0.04	0.10	0.12	0.11 ± 0.06
HD 217014	5804 ± 36	4.42 ± 0.07	1.20 ± 0.05	0.20 ± 0.05	0.08	0.07	0.08 ± 0.07
HD 217107	5645 ± 00	4.31 ± 0.00	1.06 ± 0.00	0.37 ± 0.00	0.15	0.07	0.11 ± 0.06
HD 222582	5843 ± 38	4.45 ± 0.07	1.03 ± 0.06	0.05 ± 0.05	0.09	0.09	0.09 ± 0.07

Table 11: Cu abundances from CuI lines at 5218 Å and 5782 Å a for a set of comparison stars.

Star	$T_{\rm eff}$ (K)	$\log g$ (cm s^{-2})	ξ_t (km s^{-1})	[Fe/H]	[Cu/Fe]$_1$	[Cu/Fe]$_2$	[Cu/Fe]
HD 1581	5956 ± 44	4.39 ± 0.13	1.07 ± 0.09	−0.14 ± 0.05	−0.01	0.03	0.01 ± 0.07
HD 4391	5878 ± 53	4.74 ± 0.15	1.13 ± 0.10	−0.03 ± 0.06	0.00	0.01	0.01 ± 0.08
HD 5133	4911 ± 54	4.49 ± 0.18	0.71 ± 0.11	−0.17 ± 0.06	0.05	0.00	0.03 ± 0.08
HD 7570	6140 ± 41	4.39 ± 0.16	1.50 ± 0.08	0.18 ± 0.05	0.05	0.09	0.07 ± 0.07
HD 10360	4970 ± 40	4.49 ± 0.10	0.76 ± 0.07	−0.26 ± 0.04	0.01	−0.03	−0.01 ± 0.07
HD 10700	5344 ± 29	4.57 ± 0.09	0.91 ± 0.06	−0.52 ± 0.04	0.02	−0.03	−0.01 ± 0.07
HD 14412	5368 ± 24	4.55 ± 0.05	0.88 ± 0.05	−0.47 ± 0.03	0.05	0.00	0.03 ± 0.06
HD 17925	5180 ± 56	4.44 ± 0.13	1.33 ± 0.08	0.06 ± 0.07	0.00	−0.10	−0.05 ± 0.09
HD 20010	6275 ± 57	4.40 ± 0.37	2.41 ± 0.41	−0.19 ± 0.06	−0.05	0.09	0.02 ± 0.14
HD 20766	5733 ± 31	4.55 ± 0.10	1.09 ± 0.06	−0.21 ± 0.04	0.05	0.02	0.04 ± 0.07
HD 20794	5444 ± 31	4.47 ± 0.07	0.98 ± 0.06	−0.38 ± 0.04	0.10	0.09	0.10 ± 0.06
HD 20807	5843 ± 26	4.47 ± 0.10	1.17 ± 0.06	−0.23 ± 0.04	0.00	0.02	0.01 ± 0.06
HD 23249	5074 ± 60	3.77 ± 0.16	1.08 ± 0.06	0.13 ± 0.08	0.18	0.12	0.15 ± 0.09
HD 23356	4975 ± 55	4.48 ± 0.16	0.77 ± 0.09	−0.11 ± 0.06	0.16	0.08	0.12 ± 0.09
HD 23484	5176 ± 45	4.41 ± 0.17	1.03 ± 0.06	0.06 ± 0.05	0.00	−0.10	−0.05 ± 0.09
HD 26965	5126 ± 34	4.51 ± 0.08	0.60 ± 0.07	−0.31 ± 0.04	0.12	0.07	0.10 ± 0.07
HD 30495	5868 ± 30	4.55 ± 0.10	1.24 ± 0.05	0.02 ± 0.04	−0.05	0.03	−0.01 ± 0.07
HD 36435	5479 ± 37	4.61 ± 0.07	1.12 ± 0.05	0.00 ± 0.05	−0.12	−0.08	−0.10 ± 0.07
HD 38858	5752 ± 32	4.53 ± 0.07	1.26 ± 0.07	−0.23 ± 0.05	−0.03	0.00	−0.01 ± 0.07
HD 40307	4805 ± 52	4.37 ± 0.37	0.49 ± 0.12	−0.30 ± 0.05	0.00	−0.05	−0.02 ± 0.09
HD 43162	5633 ± 35	4.48 ± 0.07	1.24 ± 0.05	−0.01 ± 0.04	−0.12	−0.14	−0.13 ± 0.06
HD 43834	5594 ± 36	4.41 ± 0.09	1.05 ± 0.04	0.10 ± 0.05	0.15	0.10	0.13 ± 0.07
HD 50281	4658 ± 56	4.32 ± 0.24	0.64 ± 0.15	−0.04 ± 0.07	0.00	−0.03	−0.01 ± 0.09
HD 53705	5825 ± 20	4.37 ± 0.10	1.20 ± 0.04	−0.19 ± 0.03	0.01	0.04	0.02 ± 0.06
HD 53706	5260 ± 31	4.35 ± 0.11	0.74 ± 0.05	−0.26 ± 0.04	0.10	0.04	0.07 ± 0.07
HD 65907	5979 ± 31	4.59 ± 0.12	1.36 ± 0.10	−0.29 ± 0.04	0.08	0.10	0.09 ± 0.07
HD 69830	5410 ± 26	4.38 ± 0.07	0.89 ± 0.03	−0.03 ± 0.04	0.05	−0.03	0.01 ± 0.07
HD 72673	5242 ± 28	4.50 ± 0.09	0.69 ± 0.05	−0.37 ± 0.04	0.07	0.04	0.06 ± 0.06
HD 74576	5000 ± 55	4.55 ± 0.13	1.07 ± 0.08	−0.03 ± 0.06	−0.05	−0.11	−0.08 ± 0.08
HD 76151	5803 ± 29	4.50 ± 0.08	1.02 ± 0.04	0.14 ± 0.04	0.03	−0.01	0.01 ± 0.06
HD 84117	6167 ± 37	4.35 ± 0.10	1.42 ± 0.09	−0.03 ± 0.05	−0.05	0.01	−0.02 ± 0.07
HD 189567	5765 ± 24	4.52 ± 0.05	1.22 ± 0.05	−0.23 ± 0.04	0.05	0.04	0.05 ± 0.06
HD 191408	5005 ± 45	4.38 ± 0.25	0.67 ± 0.09	−0.55 ± 0.06	0.15	0.12	0.14 ± 0.08

Table 11: Continued.

Star	$T_{\rm eff}$ (K)	$\log g$ (cm s^{-2})	ξ_t (km s^{-1})	[Fe/H]	[Cu/Fe]$_1$	[Cu/Fe]$_2$	[Cu/Fe]
HD 192310	5069 ± 49	4.38 ± 0.19	0.79 ± 0.07	−0.01 ± 0.05	0.18	0.07	0.13 ± 0.09
HD 196761	5435 ± 39	4.48 ± 0.08	0.91 ± 0.07	−0.29 ± 0.05	0.02	0.04	0.03 ± 0.07
HD 207129	5910 ± 24	4.42 ± 0.05	1.14 ± 0.04	0.00 ± 0.04	−0.07	−0.05	−0.06 ± 0.06
HD 209100	4629 ± 77	4.36 ± 0.19	0.42 ± 0.25	−0.06 ± 0.08	0.02	−0.13	−0.06 ± 0.13
HD 211415	5890 ± 30	4.51 ± 0.07	1.12 ± 0.07	−0.17 ± 0.04	−0.02	0.04	0.01 ± 0.07
HD 216803	4555 ± 87	4.53 ± 0.26	0.66 ± 0.28	−0.01 ± 0.09	−0.01	−0.07	−0.04 ± 0.12
HD 222237	4747 ± 58	4.48 ± 0.22	0.40 ± 0.20	−0.31 ± 0.06	0.21	0.11	0.16 ± 0.10
HD 222335	5260 ± 41	4.45 ± 0.11	0.92 ± 0.06	−0.16 ± 0.05	0.01	0.03	0.02 ± 0.07

Table 12: Average [X/H] values, with the corresponding dispersions, for the set of planet host stars and the comparison sample.

Species	<[X/H]> ± rms (comp. sample)	<[X/H]> ± rms (planet hosts)	Difference
C	−0.03 ± 0.14	0.14 ± 0.17	0.17
S	−0.18 ± 0.14	−0.02 ± 0.17	0.16
Zn	−0.12 ± 0.16	0.13 ± 0.22	0.25
Cu	−0.12 ± 0.17	0.19 ± 0.23	0.31

Table 13: Comparison of measured *EW* of C I line at 5380 Å from our data and from other authors.

Star	$T_{\rm eff}$ (K)	$\log g$ (cm s^{-2})	ξ_t (km s^{-1})	[Fe/H]	EW	EW$_{liter}$	Ref.
HD 1237	5536 ± 50	4.56 ± 0.12	1.33 ± 0.06	0.12 ± 0.06	16.7	17.0	1
HD 9826	6212 ± 64	4.26 ± 0.13	1.69 ± 0.16	0.13 ± 0.08	45.2	41.5	3
HD 10697	5641 ± 28	4.05 ± 0.05	1.13 ± 0.03	0.14 ± 0.04	27.4	24.9	2
HD 12661	5702 ± 36	4.33 ± 0.08	1.05 ± 0.04	0.36 ± 0.05	32.3	31.9	2K
HD 13445	5163 ± 00	4.52 ± 0.00	0.72 ± 0.00	−0.24 ± 0.00	12.9	7.8	1
HD 22049	5073 ± 42	4.43 ± 0.08	1.05 ± 0.06	−0.13 ± 0.05	9.5	9.8	3
HD 37124	5546 ± 30	4.50 ± 0.03	0.80 ± 0.07	−0.38 ± 0.04	13.0	11.9	2K
HD 38529	5674 ± 40	3.94 ± 0.12	1.38 ± 0.05	0.40 ± 0.06	45.0	35.2	2K
HD 38529	5674 ± 40	3.94 ± 0.12	1.38 ± 0.05	0.40 ± 0.06	45.0	35.5	3
HD 46375	5268 ± 55	4.41 ± 0.16	0.97 ± 0.06	0.20 ± 0.06	20.8	19.7	2K
HD 52265	6105 ± 00	4.28 ± 0.00	1.36 ± 0.00	0.23 ± 0.00	43.6	39.4	1
HD 52265	6105 ± 00	4.28 ± 0.00	1.36 ± 0.00	0.23 ± 0.06	43.6	41.6	2K
HD 52265	6105 ± 00	4.28 ± 0.00	1.36 ± 0.00	0.23 ± 0.06	43.6	37.1	3
HD 75289	6143 ± 53	4.42 ± 0.13	1.53 ± 0.09	0.28 ± 0.07	37.6	39.0	1
HD 75732	5279 ± 62	4.37 ± 0.18	0.98 ± 0.07	0.33 ± 0.07	21.6	19.5	3
HD 82943	6015 ± 00	4.46 ± 0.00	1.13 ± 0.00	0.30 ± 0.00	37.6	35.4	4
HD 82943	6015 ± 00	4.46 ± 0.00	1.13 ± 0.00	0.30 ± 0.00	37.6	36.3	1
HD 83443	5454 ± 61	4.33 ± 0.17	1.08 ± 0.08	0.35 ± 0.08	27.7	26.1	1
HD 89744	6234 ± 45	3.98 ± 0.05	1.62 ± 0.08	0.22 ± 0.05	50.2	49.3	2
HD 89744	6234 ± 45	3.98 ± 0.05	1.62 ± 0.08	0.22 ± 0.05	50.2	43.0	3
HD 92788	5821 ± 41	4.45 ± 0.06	1.16 ± 0.05	0.32 ± 0.05	37.0	31.1	2K
HD 92788	5821 ± 41	4.45 ± 0.06	1.16 ± 0.05	0.32 ± 0.05	37.0	28.8	4
HD 95128	5954 ± 25	4.44 ± 0.10	1.30 ± 0.04	0.06 ± 0.03	25.9	25.8	3
HD 106252	5899 ± 35	4.34 ± 0.07	1.08 ± 0.06	−0.01 ± 0.05	23.1	21.8	4
HD 114762	5884 ± 34	4.22 ± 0.22	1.31 ± 0.17	−0.70 ± 0.04	12.2	10.0	4
HD 117176	5560 ± 34	4.07 ± 0.05	1.18 ± 0.05	−0.06 ± 0.05	18.0	14.9	3

Table 13: Continued.

Star	$T_{\rm eff}$ (K)	$\log g$ (cm s^{-2})	ξ_t (km s^{-1})	[Fe/H]	EW	EW$_{liter}$	Ref.
HD 120136	6339 ± 73	4.19 ± 0.10	1.70 ± 0.16	0.23 ± 0.07	59.9	56.8	3
HD 130322	5392 ± 36	4.48 ± 0.06	0.85 ± 0.05	0.03 ± 0.04	14.5	14.6	2
HD 130322	5392 ± 36	4.48 ± 0.06	0.85 ± 0.05	0.03 ± 0.04	14.5	13.7	4
HD 134987	5776 ± 29	4.36 ± 0.07	1.09 ± 0.04	0.30 ± 0.04	36.3	34.8	2
HD 134987	5776 ± 29	4.36 ± 0.07	1.09 ± 0.04	0.30 ± 0.04	36.3	34.1	4
HD 141937	5909 ± 39	4.51 ± 0.08	1.13 ± 0.06	0.10 ± 0.05	28.2	26.5	4
HD 143761	5853 ± 25	4.41 ± 0.15	1.35 ± 0.07	−0.21 ± 0.04	21.1	15.9	3
HD 145675	5311 ± 87	4.42 ± 0.18	0.92 ± 0.10	0.43 ± 0.08	24.5	23.9	3
HD 168443	5617 ± 35	4.22 ± 0.05	1.21 ± 0.05	0.06 ± 0.05	26.7	27.3	2
HD 168746	5601 ± 33	4.41 ± 0.12	0.99 ± 0.05	−0.08 ± 0.05	22.5	18.0	4
HD 169830	6299 ± 41	4.10 ± 0.02	1.42 ± 0.09	0.21 ± 0.05	48.2	45.1	1
HD 186427	5772 ± 25	4.40 ± 0.07	1.07 ± 0.04	0.08 ± 0.04	23.8	23.9	3
HD 187123	5845 ± 22	4.42 ± 0.07	1.10 ± 0.03	0.13 ± 0.03	26.2	24.9	4
HD 190228	5325 ± 00	3.90 ± 0.00	1.11 ± 0.00	−0.26 ± 0.00	12.6	11.9	4
HD 202206	5752 ± 53	4.50 ± 0.09	1.01 ± 0.06	0.35 ± 0.06	27.1	22.5	1
HD 217014	5804 ± 36	4.42 ± 0.07	1.20 ± 0.05	0.20 ± 0.05	34.3	30.2	2
HD 217014	5804 ± 36	4.42 ± 0.07	1.20 ± 0.05	0.20 ± 0.05	34.3	29.5	3
HD 217107	5645 ± 00	4.31 ± 0.00	1.06 ± 0.00	0.37 ± 0.00	29.1	27.6	2
HD 217107	5645 ± 00	4.31 ± 0.00	1.06 ± 0.00	0.37 ± 0.00	29.1	29.4	3
HD 222582	5843 ± 38	4.45 ± 0.07	1.03 ± 0.06	0.05 ± 0.05	22.2	20.1	2

[1] from Santos et al. (2000)
[2] from Gonzalez et al. (2001); 2K refers to data from Keck spectra
[3] from Takeda et al. (2001)
[4] from Sadakane et al. (2002)

Table 14: Comparison of sulphur abundances from our results and from other authors.

Star	$T_{\rm eff}$ (K)	$\log g$ (cm s^{-2})	ξ_t (km s^{-1})	[Fe/H]	[S/Fe]	[S/Fe]$_{liter}$	Ref.
HD 1237	5536 ± 50	4.56 ± 0.12	1.33 ± 0.06	0.12 ± 0.06	−0.22 ± 0.08	0.00	1
HD 9826	6212 ± 64	4.26 ± 0.13	1.69 ± 0.16	0.13 ± 0.08	−0.33 ± 0.09	0.06	2
HD 22049	5073 ± 42	4.43 ± 0.08	1.05 ± 0.06	−0.13 ± 0.05	0.00 ± 0.08	0.32	2
HD 38529	5674 ± 40	3.94 ± 0.12	1.38 ± 0.05	0.40 ± 0.06	−0.32 ± 0.08	0.08	2
HD 52265	6105 ± 00	4.28 ± 0.00	1.36 ± 0.00	0.23 ± 0.00	−0.20 ± 0.06	0.06	2
HD 52265	6105 ± 00	4.28 ± 0.00	1.36 ± 0.00	0.23 ± 0.06	−0.20 ± 0.06	−0.12	1
HD 75289	6143 ± 53	4.42 ± 0.13	1.53 ± 0.09	0.28 ± 0.07	−0.31 ± 0.09	−0.21	1
HD 75732	5279 ± 62	4.37 ± 0.18	0.98 ± 0.07	0.33 ± 0.07	−0.20 ± 0.10	0.13	2
HD 82943	6015 ± 00	4.46 ± 0.00	1.13 ± 0.00	0.30 ± 0.00	−0.20 ± 0.05	−0.13	1
HD 82943	6015 ± 00	4.46 ± 0.00	1.13 ± 0.00	0.30 ± 0.00	−0.20 ± 0.05	−0.04	3
HD 83443	5454 ± 61	4.33 ± 0.17	1.08 ± 0.08	0.35 ± 0.08	−0.15 ± 0.10	0.07	1
HD 92788	5821 ± 41	4.45 ± 0.06	1.16 ± 0.05	0.32 ± 0.05	−0.22 ± 0.07	−0.10	3
HD 95128	5954 ± 25	4.44 ± 0.10	1.30 ± 0.04	0.06 ± 0.03	−0.26 ± 0.06	−0.08	2
HD 106252	5899 ± 35	4.34 ± 0.07	1.08 ± 0.06	−0.01 ± 0.05	−0.09 ± 0.07	−0.05	3
HD 114762	5884 ± 34	4.22 ± 0.22	1.31 ± 0.17	−0.70 ± 0.04	0.15 ± 0.09	0.12	3
HD 117176	5560 ± 34	4.07 ± 0.05	1.18 ± 0.05	−0.06 ± 0.05	0.03 ± 0.10	0.10	2
HD 120136	6339 ± 73	4.19 ± 0.10	1.70 ± 0.16	0.23 ± 0.07	−0.18 ± 0.09	0.26	2
HD 130322	5392 ± 36	4.48 ± 0.06	0.85 ± 0.05	0.03 ± 0.04	−0.06 ± 0.07	0.01	3
HD 134987	5776 ± 29	4.36 ± 0.07	1.09 ± 0.04	0.30 ± 0.04	−0.17 ± 0.07	−0.01	3
HD 141937	5909 ± 39	4.51 ± 0.08	1.13 ± 0.06	0.10 ± 0.05	−0.18 ± 0.07	0.06	3
HD 143761	5853 ± 25	4.41 ± 0.15	1.35 ± 0.07	−0.21 ± 0.04	−0.04 ± 0.07	0.15	2

Table 14: Continued.

Star	$T_{\rm eff}$ (K)	$\log g$ (cm s^{-2})	ξ_t (km s^{-1})	[Fe/H]	[S/Fe]	[S/Fe]$_{liter}$	Ref.
HD 145675	5311 ± 87	4.42 ± 0.18	0.92 ± 0.10	0.43 ± 0.08	−0.13 ± 0.12	0.32	2
HD 168746	5601 ± 33	4.41 ± 0.12	0.99 ± 0.05	−0.08 ± 0.05	0.13 ± 0.07	0.08	3
HD 169830	6299 ± 41	4.10 ± 0.02	1.42 ± 0.09	0.21 ± 0.05	−0.31 ± 0.06	−0.17	1
HD 186427	5772 ± 25	4.40 ± 0.07	1.07 ± 0.04	0.08 ± 0.04	−0.13 ± 0.06	−0.09	2
HD 187123	5845 ± 22	4.42 ± 0.07	1.10 ± 0.03	0.13 ± 0.03	−0.23 ± 0.08	−0.09	3
HD 190228	5325 ± 00	3.90 ± 0.00	1.11 ± 0.00	−0.26 ± 0.00	0.01 ± 0.07	−0.06	3
HD 202206	5752 ± 53	4.50 ± 0.09	1.01 ± 0.06	0.35 ± 0.06	−0.22 ± 0.08	−0.26	1
HD 209458	6117 ± 26	4.48 ± 0.08	1.40 ± 0.06	0.02 ± 0.03	−0.22 ± 0.06	0.00	3
HD 217014	5804 ± 36	4.42 ± 0.07	1.20 ± 0.05	0.20 ± 0.05	−0.12 ± 0.07	−0.01	2
HD 217107	5645 ± 00	4.31 ± 0.00	1.06 ± 0.00	0.37 ± 0.00	−0.24 ± 0.06	0.07	2

[1] from Santos et al. (2000)
[2] from Takeda et al. (2001)
[3] from Sadakane et al. (2002)

Table 15: Comparison of zinc abundances from our results and from other authors.

Star	$T_{\rm eff}$ (K)	$\log g$ (cm s^{-2})	ξ_t (km s^{-1})	[Fe/H]	[Zn/Fe]	[Zn/Fe]$_{liter}$	Ref.
HD 9826	6212 ± 64	4.26 ± 0.13	1.69 ± 0.16	0.13 ± 0.08	−0.12 ± 0.10	0.05	1
HD 22049	5073 ± 42	4.43 ± 0.08	1.05 ± 0.06	−0.13 ± 0.05	−0.12 ± 0.08	−0.16	1
HD 38529	5674 ± 40	3.94 ± 0.12	1.38 ± 0.05	0.40 ± 0.06	−0.14 ± 0.08	0.38	1
HD 52265	6105 ± 00	4.28 ± 0.00	1.36 ± 0.00	0.23 ± 0.00	−0.09 ± 0.07	0.14	1
HD 75732	5279 ± 62	4.37 ± 0.18	0.98 ± 0.07	0.33 ± 0.07	0.16 ± 0.09	0.48	1
HD 92788	5821 ± 41	4.45 ± 0.06	1.16 ± 0.05	0.32 ± 0.05	0.11 ± 0.07	0.29	2
HD 95128	5954 ± 25	4.44 ± 0.10	1.30 ± 0.04	0.06 ± 0.03	0.00 ± 0.07	0.11	1
HD 106252	5899 ± 35	4.34 ± 0.07	1.08 ± 0.06	−0.01 ± 0.05	−0.13 ± 0.07	−0.12	2
HD 130322	5392 ± 36	4.48 ± 0.06	0.85 ± 0.05	0.03 ± 0.04	0.06 ± 0.13	0.01	2
HD 134987	5776 ± 29	4.36 ± 0.07	1.09 ± 0.04	0.30 ± 0.04	0.19 ± 0.07	0.31	2
HD 141937	5909 ± 39	4.51 ± 0.08	1.13 ± 0.06	0.10 ± 0.05	−0.02 ± 0.08	0.05	2
HD 143761	5853 ± 25	4.41 ± 0.15	1.35 ± 0.07	−0.21 ± 0.04	0.10 ± 0.08	−0.10	1
HD 145675	5311 ± 87	4.42 ± 0.18	0.92 ± 0.10	0.43 ± 0.08	0.16 ± 0.11	0.54	1
HD 168746	5601 ± 33	4.41 ± 0.12	0.99 ± 0.05	−0.08 ± 0.05	0.14 ± 0.08	0.02	2
HD 186427	5772 ± 25	4.40 ± 0.07	1.07 ± 0.04	0.08 ± 0.04	0.11 ± 0.06	−0.03	1
HD 187123	5845 ± 22	4.42 ± 0.07	1.10 ± 0.03	0.13 ± 0.03	0.08 ± 0.06	0.08	2
HD 192263	4947 ± 58	4.51 ± 0.20	0.86 ± 0.09	−0.02 ± 0.06	0.07 ± 0.09	0.12	2
HD 217014	5804 ± 36	4.42 ± 0.07	1.20 ± 0.05	0.20 ± 0.05	−0.02 ± 0.07	0.18	1
HD 217107	5645 ± 00	4.31 ± 0.00	1.06 ± 0.00	0.37 ± 0.00	0.04 ± 0.07	0.27	1

[1] from Takeda et al. (2001)
[2] from Sadakane et al. (2002)

Table 16: Comparison of copper abundances from our results and from other authors .

Star	$T_{\rm eff}$ (K)	$\log g$ (cm s^{-2})	ξ_t (km s^{-1})	[Fe/H]	[Cu/Fe]	[Cu/Fe]$_{liter}$	Ref.
HD 92788	5821 ± 41	4.45 ± 0.06	1.16 ± 0.05	0.32 ± 0.05	0.19 ± 0.07	0.52	1
HD 106252	5899 ± 35	4.34 ± 0.07	1.08 ± 0.06	−0.01 ± 0.05	−0.02 ± 0.07	−0.04	1
HD 130322	5392 ± 36	4.48 ± 0.06	0.85 ± 0.05	0.03 ± 0.04	0.03 ± 0.07	0.16	1

Table 16: Continued.

Star	$T_{\rm eff}$ (K)	$\log g$ (cm s^{-2})	ξ_t (km s^{-1})	[Fe/H]	[Cu/Fe]	[Cu/Fe]$_{liter}$	Ref.
HD 134987	5776 ± 29	4.36 ± 0.07	1.09 ± 0.04	0.30 ± 0.04	0.19 ± 0.06	0.52	1
HD 141937	5909 ± 39	4.51 ± 0.08	1.13 ± 0.06	0.10 ± 0.05	0.07 ± 0.07	0.13	1
HD 168746	5601 ± 33	4.41 ± 0.12	0.99 ± 0.05	−0.08 ± 0.05	0.10 ± 0.07	0.03	1
HD 187123	5845 ± 22	4.42 ± 0.07	1.10 ± 0.03	0.13 ± 0.03	0.07 ± 0.06	0.20	1
HD 192263	4947 ± 58	4.51 ± 0.20	0.86 ± 0.09	−0.02 ± 0.06	0.01 ± 0.08	0.04	1

[1] from Sadakane et al. (2002)